

Analysing the charged scalar boson contribution to the charged-current B meson anomalies

Jonathan Cardozo,^{1,*} J. H. Muñoz,^{1,†} Néstor Quintero,^{2,‡} and Eduardo Rojas^{3,§}

¹*Departamento de Física, Universidad del Tolima, Código Postal 730006299, Ibagué, Colombia*

²*Facultad de Ciencias Básicas, Universidad Santiago de Cali, Campus Pampalinda,
Calle 5 No. 62-00, Código Postal 76001, Santiago de Cali, Colombia*

³*Departamento de Física, Universidad de Nariño, A.A. 1175, San Juan de Pasto, Colombia*

Experimental measurements collected by the BABAR, Belle, and LHCb experiments on different observables associated with the semileptonic transition $b \rightarrow c\tau\bar{\nu}_\tau$, indicate the existence of disagreement respect with the Standard Model predictions. These so-called charged-current B meson anomalies include the eight years long-standing discrepancies on $R(D)$ and $R(D^*)$, together with $R(J/\psi)$ and the polarizations $P_\tau(D^*)$ and $F_L(D^*)$ from $\bar{B} \rightarrow D^*\tau\bar{\nu}_\tau$. We analyse the charged scalar boson contributions to these anomalies within the framework of two Higgs doublet model (2HDM) with the most general Yukawa couplings to quarks and leptons from the third generation, involving left-handed and right-handed (sterile) neutrinos. Considering the most recent data from HFLAV world-average and Belle combination, the upper limits $\text{BR}(B_c^- \rightarrow \tau^-\bar{\nu}_\tau) < 30\%$ and 10% , and the inclusive ratio $R(X_c)$, we perform a phenomenological study of the parameter space, by paying special attention to the right-handed neutrino solutions. We also include the prospect measurements on $R(D^{(*)})$ that the Belle II experiment could achieve and explore the future implications to the charged scalar boson scenario. Our results show that current experimental $b \rightarrow c\tau\bar{\nu}_\tau$ data and Belle II projection favor the interpretation of a charged scalar boson interacting with right-handed neutrinos. Additionally, as a side analysis, we revisit the relation between $R(D^*)$ and $\text{BR}(B_c^- \rightarrow \tau^-\bar{\nu}_\tau)$ by investigating whether the claim that pseudoscalar new physics interpretations of $R(D^*)$ are implausible due to the B_c lifetime is still valid, to the light of the recent data and Belle II prospects on $R(D^*)$. Lastly, we reexamine addressing the $R(D^{(*)})$ anomalies in the context of the 2HDM of Type II. We show that with the current Belle combined data is possible to obtain an available parameter space on the plane $(M_{H^\pm}, \tan\beta)$ for a simultaneous explanation of the anomalies, in consistency with $B \rightarrow \tau\bar{\nu}_\tau$ and bounds from inclusive radiative B decays. Moreover, projections at the Belle II experiment suggest that the 2HDM of Type II would be no longer disfavored.

I. INTRODUCTION

The most recent experimental information accumulated by the BABAR, Belle, and LHCb experiments on the measurements of the observables $R(D^{(*)}) = \text{BR}(B \rightarrow D^{(*)}\tau\bar{\nu}_\tau)/\text{BR}(B \rightarrow D^{(*)}\ell\bar{\nu}_\ell)$, with $\ell = \mu$ or e , $R(J/\psi) = \text{BR}(B_c \rightarrow J/\psi\tau\bar{\nu}_\tau)/\text{BR}(B_c \rightarrow J/\psi\mu\bar{\nu}_\mu)$, the τ polarization asymmetry $P_\tau(D^*)$ and the longitudinal polarization of the D^* meson $F_L(D^*)$ related with the channel $\bar{B} \rightarrow D^*\tau\bar{\nu}_\tau$ have shown deviations from their corresponding Standard Model (SM) estimations [1–18]. In Table I we summarize the current experimental measurements and the SM predictions for these observables generated by the charged-current transition $b \rightarrow c\tau\bar{\nu}_\tau$. The SM average values reported by HFLAV take into account the recent theoretical progress on the calculations of $R(D^{(*)})$ [19–22].¹ For completeness, the inclusive ratio $R(X_c) = \text{BR}(B \rightarrow X_c\tau\bar{\nu}_\tau)/\text{BR}(B \rightarrow X_c\ell\bar{\nu}_\ell)$, which is induced via the same transition $b \rightarrow c\tau\bar{\nu}_\tau$ [25], is also collected in Table I. We can see that although the $R(D^{(*)})$ discrepancies have decreased with the latest measurements of Belle, it is still interesting and worthwhile to analyse them in light of future data at Belle II, where it is expected statistical and experimental improvements on the observables $R(D^{(*)})$ [26]. These charged-current B meson anomalies pose an interesting challenge, at theoretical level, in order to propose possible scenarios of physics beyond SM according to current and future experimental results.

Several model-independent analyses of new physics (NP) explanations regarding the most general dimension-six effective Lagrangian with the current $b \rightarrow c\tau\bar{\nu}_\tau$ data have been explored [27–37]. One of the possible NP scenarios that could address the aforementioned anomalies is to consider sizeable scalar couplings that arise from a charged scalar boson. This is the case of the well known two-Higgs doublet model (2HDM) which has been widely studied [38–58]. In

* jcardozo@ut.edu.co

† jhmunoz@ut.edu.co

‡ nestor.quintero01@usc.edu.co; (Corresponding author)

§ eduro4000@gmail.com

¹ For other recent works, see, for instance [23, 24]

Observable	Expt. measurement	SM prediction
$R(D)$	$0.307 \pm 0.037 \pm 0.016$ Belle-2019 [9]	0.299 ± 0.003 [12, 13]
	0.326 ± 0.034 Belle combination [9]	
	$0.340 \pm 0.027 \pm 0.013$ HFLAV [12]	
$R(D^*)$	$0.283 \pm 0.018 \pm 0.014$ Belle-2019 [9]	0.258 ± 0.005 [12, 13]
	0.283 ± 0.018 Belle combination [9]	
	$0.295 \pm 0.011 \pm 0.008$ HFLAV [12]	
$R(J/\psi)$	$0.71 \pm 0.17 \pm 0.18$ [14]	0.283 ± 0.048 [16]
$P_\tau(D^*)$	$-0.38 \pm 0.51_{-0.16}^{+0.21}$ [10, 11]	-0.497 ± 0.013 [17]
$F_L(D^*)$	$0.60 \pm 0.08 \pm 0.035$ [15]	0.46 ± 0.04 [18]
$R(X_c)$	0.223 ± 0.030 [25]	0.216 ± 0.003 [25]

TABLE I. Experimental status and SM predictions on observables related to the charged transition $b \rightarrow c\tau\bar{\nu}_\tau$.

the situation of the 2HDM of type II, this model is not favored by the experimental results reported by the BABAR experiment in 2012 and 2013 [1, 2]. However, subsequent analysis performed by the Belle Collaboration in 2015 and 2016 [3, 4] showed compatibility with the 2HDM of Type II. In particular, in Ref. [5] was discussed the compatibility of the Belle results reported for $R(D^{(*)})$ in 2016 with the 2HDM of Type II and found that these results seem to favor the parametric space with small values of $\tan\beta/M_{H^\pm}$, where $\tan\beta$ and M_{H^\pm} are the ratio of vacuum expectation values and the charged Higgs boson mass, respectively. Thus, the 2HDM of Type II was ruled out as an interpretation of the anomalies and different versions of the 2HDM were put forward in the literature, such as, type III (generic), type X (lepton-specific), flipped, and aligned, that, in general, can provide an explanation to the $R(D^{(*)})$ anomalies under certain phenomenological assumptions [38–58]. Furthermore, the parametric space of charged scalar boson interpretations has to confront strong constraints from the upper limits on the branching ratio of the tauonic B_c decay, $\text{BR}(B_c^- \rightarrow \tau^- \bar{\nu}_\tau) \lesssim 30\%$ and 10% , which are imposed from the lifetime of B_c meson [59] and the LEP data taken at the Z peak [60], respectively.

Another perspective to explain the charged-current B meson anomalies is to assume that NP might be connected with right-handed neutrinos. In this direction, several authors have incorporated a right-handed neutrino in the most general effective Hamiltonian for the $b \rightarrow c\tau\bar{\nu}_\tau$ transition with different mediators (a charged scalar boson, a heavy charged vector boson or a leptoquark) with the purpose of exploring scenarios of NP that could explain some observables related with this transition [29, 32, 33, 57, 61–76]. With the assumption of a sterile right-handed neutrino with small mass, as a singlet of the gauge group of the SM, there is no interference between contributions of left-handed and right-handed neutrinos, so the branching ratio of $b \rightarrow c\tau\nu$ is given by an incoherent sum of these contributions: $\text{BR}(b \rightarrow c\tau\bar{\nu}_\tau) = \text{BR}(b \rightarrow c\tau\bar{\nu}_L) + \text{BR}(b \rightarrow c\tau\bar{\nu}_R)$.

In this work, we perform a systematic and general model-independent study about the impact of charged scalar contributions to the charged current transition $b \rightarrow c\tau\bar{\nu}_\tau$, including light right-handed neutrinos. The inclusion of sterile neutrinos allows additional scalar contributions in the effective Hamiltonian that could disentangle the discrepancy between experimental measurements and SM predictions for the charged-current B -meson anomalies. In our study we consider the observables $R(D^{(*)})$, $R(J/\psi)$, $P_\tau(D^*)$, $F_L(D^*)$, the inclusive $R(X_c)$, and constraints derived from the branching ratio of $B_c \rightarrow \tau\bar{\nu}_\tau$. Recently, the impact of the mentioned scalar contributions with right-handed neutrinos on several observables related with the $b \rightarrow c\tau\bar{\nu}_\tau$ transition was performed in Refs. [29, 65], exploring the parametric space of the Wilson coefficients that could explain the anomalies. In our work, we include additional elements as the projected Belle II sensitivities and a complete analysis of the parametric space of the Yukawa couplings, which is not straightforward because there is no a trivial relation among the Wilson coefficients and the Yukawa couplings. None of these previous studies [29, 65] included these relevant aspects in their analysis. In particular, the future measurements at the ongoing Belle II experiment are a matter of importance to confirm or refute the tantalizing NP hints.

Additionally, we reexamine the relation between the observable $R(D^*)$ and $\text{BR}(B_c \rightarrow \tau\bar{\nu}_\tau)$, reported in Refs. [59, 60], in light of Belle combination [9] and LHCb [7] experimental results, and the projection at Belle II experiment with an integrated luminosity of 50 ab^{-1} [26]. This analysis is very important because the constraint on $\text{BR}(B_c \rightarrow \tau\bar{\nu}_\tau)$ affects substantially the contributions from scalar operators [33–35]. We also reanalyze the parametric space ($M_{H^\pm}, \tan\beta$) in order to determine if the 2HDM of Type II is still disfavored to explain the $R(D^*)$ anomalies considering the recent experimental results of Belle [9] and the projected Belle II experiment [26].

This paper is organized as follows. In Sec. II, we present the expressions for the observables $R(D^{(*)})$, $R(J/\psi)$, $P_\tau(D^*)$, $F_L(D^*)$, $R(X_c)$ and $BR(B_c \rightarrow \tau\nu)$, in terms of the Wilson coefficients associated to scalar contributions considering left and right-handed neutrinos. In Sec. III, we perform a phenomenological analysis on the parametric space of Wilson coefficients and Yukawa couplings, considering the recent experimental results of Belle and the future projection at the Belle II experiment, to determine possible regions where scalar contributions with right-handed neutrinos could explain the charged B -meson anomalies. In Sec. IV, we dig into the relation between the $R(D^*)$ anomaly and the $BR(B_c \rightarrow \tau\bar{\nu}_\tau)$ considering constrains of 30% and 10% and the recent $b \rightarrow c\tau\bar{\nu}_\tau$ data and projected results at Belle II. In Sec. V, we reanalyze the old discussion if the 2HDM of Type II is still rule out as an interpretation to the $R(D^{(*)})$ anomalies. Our main conclusions are given in Sec. VI. Finally, in the appendix we perform a detailed phenomenological study of a general 2HDM in order to calculate the effective Yukawa couplings and the corresponding Wilson coefficients.

II. SCALAR CONTRIBUTIONS TO THE $b \rightarrow c\tau\bar{\nu}_\tau$ OBSERVABLES

The effective Hamiltonian for the charged-current transition $b \rightarrow c\tau\bar{\nu}_\tau$ that includes all the four-fermion scalar operators, considering both left- and right-handed neutrinos, has the following form [29, 61–65]

$$\begin{aligned} \mathcal{H}_{\text{eff}}(b \rightarrow c\tau\bar{\nu}_\tau) = & \frac{4G_F}{\sqrt{2}} V_{cb}^{\text{CKM}} \left[(\bar{c}\gamma_\mu P_L b)(\bar{\tau}\gamma^\mu P_L \nu_\tau) + C_S^{LL}(\bar{c}P_L b)(\bar{\tau}P_L \nu_\tau) + C_S^{RL}(\bar{c}P_R b)(\bar{\tau}P_L \nu_\tau) \right. \\ & \left. + C_S^{LR}(\bar{c}P_L b)(\bar{\tau}P_R \nu_\tau) + C_S^{RR}(\bar{c}P_R b)(\bar{\tau}P_R \nu_\tau) \right] + h.c., \end{aligned} \quad (1)$$

where $P_{R,L} = (1 \pm \gamma_5)/2$, G_F is the Fermi coupling constant and V_{cb}^{CKM} is the charm-bottom Cabbibo-Kobayashi-Maskawa (CKM) matrix element. The first term corresponds to the SM contribution from a virtual W boson exchange, while the remaining four terms correspond to the all possible charged scalar contributions. The information of these NP operators is codify through the scalar Wilson coefficients (WCs) C_S^{XY} , where the first index $X = L, R$ represents the quark-current quirality projection, while the second one $Y = L, R$ is related with the leptonic-current quirality projection. Thus, Eq. (1) contains all of the dimension-six scalar operators involving both left-handed (LH) and right-handed (RH) neutrinos. We will assume that NP effects are only present in the third generation of leptons (τ, ν_τ). This assumption is motivated by the absence of deviations from the SM for light lepton modes $\ell = e$ or μ .

The ratios $R(M)$ ($M = D, D^*, J/\psi$), and the D^* and τ longitudinal polarizations can be written in terms of the scalar WCs C_S^{LL} , C_S^{RL} , C_S^{LR} , and C_S^{RR} [61–63]. The numerical expressions for these contributions are [61–63]:

$$R(D) = R(D)_{\text{SM}} \left[1 + 1.49 \text{Re}(C_S^{RL} + C_S^{LL})^* + 1.02(|C_S^{RL} + C_S^{LL}|^2 + |C_S^{LR} + C_S^{RR}|^2) \right], \quad (2)$$

$$R(D^*) = R(D^*)_{\text{SM}} \left[1 + 0.11 \text{Re}(C_S^{RL} - C_S^{LL})^* + 0.04(|C_S^{RL} - C_S^{LL}|^2 + |C_S^{LR} - C_S^{RR}|^2) \right], \quad (3)$$

$$R(J/\psi) = R(J/\psi)_{\text{SM}} \left[1 + 0.12 \text{Re}(C_S^{RL} - C_S^{LL})^* + 0.04(|C_S^{RL} - C_S^{LL}|^2 + |C_S^{LR} - C_S^{RR}|^2) \right], \quad (4)$$

$$F_L(D^*) = F_L(D^*)_{\text{SM}} r_{D^*}^{-1} \left[1 + 0.24 \text{Re}(C_S^{RL} - C_S^{LL})^* + 0.08(|C_S^{RL} - C_S^{LL}|^2 + |C_S^{LR} - C_S^{RR}|^2) \right], \quad (5)$$

$$P_\tau(D^*) = P_\tau(D^*)_{\text{SM}} r_{D^*}^{-1} \left[1 - 0.22 \text{Re}(C_S^{RL} - C_S^{LL})^* - 0.07(|C_S^{RL} - C_S^{LL}|^2 + |C_S^{LR} - C_S^{RR}|^2) \right], \quad (6)$$

with $r_{D^*} = R(D^*)/R(D^*)_{\text{SM}}$. The numerical formula for $R(J/\psi)$ has been obtained by using the analytic expressions and form factors given in Ref. [16]. Similarly, the tauonic decay $B_c^- \rightarrow \tau^- \bar{\nu}_\tau$ is also modified as follows [61–63]

$$\text{BR}(B_c^- \rightarrow \tau^- \bar{\nu}_\tau) = \text{BR}(B_c^- \rightarrow \tau^- \bar{\nu}_\tau)_{\text{SM}} \left[\left| 1 + \frac{m_{B_c}^2}{m_\tau(m_b + m_c)} (C_S^{RL} - C_S^{LL}) \right|^2 + \left| \frac{m_{B_c}^2}{m_\tau(m_b + m_c)} (C_S^{LR} - C_S^{RR}) \right|^2 \right], \quad (7)$$

where $m_{B_c}^2/m_\tau(m_b + m_c) = 4.33$. Finally, the ratio $R(X_c)$ of inclusive semileptonic B decays in the $1S$ scheme can be written as [25]

$$\begin{aligned} R(X_c) = R(X_c)_{\text{SM}} & \left[1 + 0.096 \text{Re}(C_S^{RL} - C_S^{LL})^* + 0.493 \text{Re}(C_S^{RL} + C_S^{LL})^* \right. \\ & \left. + 0.031(|C_S^{RL} - C_S^{LL}|^2 + |C_S^{LR} - C_S^{RR}|^2) + 0.327(|C_S^{RL} + C_S^{LL}|^2 + |C_S^{LR} + C_S^{RR}|^2) \right]. \end{aligned} \quad (8)$$

This formula was obtained by following the trick described in Ref. [62], in which the contributions of scalar Wilson coefficients with RH neutrinos are calculated by using parity transformation ($L \leftrightarrow R$). Without loss of generality, in the following, we will restrict our analysis to the case of real scalar WCs².

III. PHENOMENOLOGICAL ANALYSIS

Before to addressing the charged-current B meson anomalies in terms of scalar WCs, it is necessary to discuss the present-day experimental measurements on the ratios $R(D)$ and $R(D^*)$ (see Table I). The most recent world-average values reported by the Heavy Flavor Averaging Group (HFLAV) on the measurements of $R(D)$ and $R(D^*)$ [12, 13] exceed the SM predictions by 1.4σ and 2.5σ , respectively. These averages include the Belle Collaboration measurements released in 2019 [9], which are in agreement with the SM predictions within 0.2σ and 1.1σ , respectively. Furthermore, the Belle combination averages on $R(D^{(*)})$ are in accordance with the SM within 0.8σ and 1.4σ , respectively [9]. Given this current experimental situation and the importance of Belle efforts to improve the measurements on $R(D^{(*)})$, we will consider in our analysis two different sets of observables, namely

- Set 1 (S1): $R(D^{(*)})$ HFLAV, $R(J/\psi)$, $F_L(D^*)$, $P_\tau(D^*)$, $R(X_c)$,
- Set 2 (S2): $R(D^{(*)})$ Belle combination, $R(J/\psi)$, $F_L(D^*)$, $P_\tau(D^*)$, $R(X_c)$,

where the corresponding theoretical and experimental values are given in Table I. The purpose of these two sets is to observe the significance of the recent HFLAV world-average and Belle combination data [9, 12, 13], as well as to provide a robust analysis by regarding the available experimental information on all of the charged transition $b \rightarrow c\tau\bar{\nu}_\tau$ observables, namely the ratios $R(J/\psi)$, $R(X_c)$, and the polarizations $P_\tau(D^*)$, $F_L(D^*)$ reported by Belle [10, 11, 15]. Moreover, we will consider into the analysis the upper bounds $\text{BR}(B_c^- \rightarrow \tau^-\bar{\nu}_\tau) < 30\%$ [59] and 10% [60] to put constraints on the scalar NP scenarios. Keeping this in mind, we determine the regions in the parameter space favored by the experimental data for the set of observables S1 and S2.

Projected Belle II scenarios

Within the physics program of the Belle II experiment [26] is expected that improvements at the level of $\sim 3\%$ and $\sim 2\%$ will be achieved, for the statistical and systematic uncertainties of $R(D)$ and $R(D^*)$, respectively. Taking into account in our analysis the projected uncertainties on $R(D^{(*)})$ when an integrated luminosity of 50 ab^{-1} data will be accumulated [26] and assuming the current Belle combination $R(D)$ - $R(D^*)$ correlation ($\rho = -0.47$ [9]), we also examine the prospects of Belle II by considering two benchmark projected scenarios, i.e., plausible scenarios within the reach and capability of Belle II. These two scenarios are:

1. **Belle II-P1:** Belle II measurements on $R(D^{(*)})$ keep the central values of Belle combination averages with the projected Belle II sensitivities for 50 ab^{-1} .
2. **Belle II-P2:** Belle II measurements on $R(D^{(*)})$ are in agreement with the current SM predictions at the 0.1σ level with the projected Belle II sensitivities for 50 ab^{-1} .

These scenarios were previously considered in the analysis of Ref. [63], but considering the HFLAV 2018 world-average values. Here, we will re-examine them based on the most recent Belle data.

Fit procedure

We carry out a standard χ^2 analysis with the above-mentioned \mathcal{O}_i observables associated with the transition $b \rightarrow c\tau\bar{\nu}_\tau$. The χ^2 function is written as [77]

$$\chi^2(C_S^{XY}) = \sum_{i,j}^{N_{\text{obs}}} [\mathcal{O}_i^{\text{exp}} - \mathcal{O}_i^{\text{th}}(C_S^{XY})] C_{ij}^{-1} [\mathcal{O}_j^{\text{exp}} - \mathcal{O}_j^{\text{th}}(C_S^{XY})], \quad (9)$$

² In Ref. [28] has been shown that the case of complex WCs do not provide an improvement in the description of the data.

Set S1 ($\chi_{\text{SM}}^2 = 19.1$, $p\text{-value}_{\text{SM}} = 7.6 \times 10^{-4}$)					
Two scalar WCs	BFP	$p\text{-value}$ (%)	pull_{SM}	1σ intervals	
(C_S^{LL}, C_S^{RL})	(-1.28,-0.25)	48.5	2.69	$C_S^{LL} \in [-1.33, -1.22]$	$C_S^{RL} \in [-0.30, -0.18]$
(C_S^{LL}, C_S^{LR})	(-0.91,-0.78)	46.8	2.68	$C_S^{LL} \in [-1.04, -0.68]$	$C_S^{LR} \in [-0.83, -0.71]$
(C_S^{LL}, C_S^{RR})	(-0.91,-0.78)	46.8	2.68	$C_S^{LL} \in [-1.04, -0.68]$	$C_S^{RR} \in [-0.83, -0.71]$
(C_S^{LR}, C_S^{RR})	(1.15,-0.82)	44.1	2.64	$C_S^{LR} \in [1.02, 1.25]$	$C_S^{RR} \in [-1.04, -0.70]$
Set S2 ($\chi_{\text{SM}}^2 = 11.2$, $p\text{-value}_{\text{SM}} = 2.4 \times 10^{-2}$)					
Two scalar WCs	BFP	$p\text{-value}$ (%)	pull_{SM}	1σ intervals	
(C_S^{LL}, C_S^{RL})	(-1.22,-0.21)	50.3	1.31	$C_S^{LL} \in [-1.29, -1.14]$	$C_S^{RL} \in [-0.30, -0.11]$
(C_S^{LL}, C_S^{LR})	(-0.92,-0.68)	49.3	1.30	$C_S^{LL} \in [-1.07, -0.55]$	$C_S^{LR} \in [-0.75, -0.59]$
(C_S^{LL}, C_S^{RR})	(-0.92,-0.68)	49.3	1.30	$C_S^{LL} \in [-1.07, -0.55]$	$C_S^{RR} \in [-0.75, -0.59]$
(C_S^{LR}, C_S^{RR})	(0.95,-0.95)	45.7	1.24	$C_S^{LR} \in [0.63, 1.18]$	$C_S^{RR} \in [-1.18, -0.63]$

TABLE II. Best-fit point (BFP) values, p -value, pull_{SM} , and 1σ allowed intervals by allowing two scalar WCs different from zero to fit the set of observables S1 and S2.

Belle II-P1			
Two scalar WCs	1σ intervals		
(C_S^{LL}, C_S^{RL})	$C_S^{LL} \in [-1.11, -1.06]$	$C_S^{RL} \in [-0.41, -0.36]$	
(C_S^{LL}, C_S^{LR})	$C_S^{LL} \in [-0.69, -0.49]$	$C_S^{LR} \in [-0.75, -0.71]$	
(C_S^{LL}, C_S^{RR})	$C_S^{LL} \in [-0.69, -0.49]$	$C_S^{RR} \in [-0.75, -0.71]$	
(C_S^{LR}, C_S^{RR})	$C_S^{LR} \in [0.69, 0.93]$ $C_S^{RR} \in [-0.84, -0.61]$		
Belle II-P2			
Two scalar WCs	1σ intervals		
(C_S^{LL}, C_S^{RL})	$C_S^{LL} \in [-0.77, -0.72]$	$C_S^{RL} \in [-0.73, -0.69]$	
(C_S^{LL}, C_S^{LR})	$C_S^{LL} \in [-0.04, 8 \times 10^{-4}]$	$C_S^{LR} \in [-0.26, -0.05]$	
(C_S^{LL}, C_S^{RR})	$C_S^{LL} \in [-0.02, 8 \times 10^{-4}]$	$C_S^{RR} \in [-0.26, -0.05]$	
(C_S^{LR}, C_S^{RR})	$C_S^{LR} \in [-5 \times 10^{-3}, 0.38]$ $C_S^{RR} \in [-0.32, 0.06]$		

TABLE III. Projections Belle II-P1 and Belle-P2 of the 1σ allowed intervals for two scalar WCs different from zero.

where N_{obs} is the number of observables, $\mathcal{O}_i^{\text{exp}}$ are the experimental measurements, and $\mathcal{O}_i^{\text{th}}$ are the theoretical observables, Eqs. (2)-(6) and (8), which are function of the scalar WCs C_S^{XY} ($XY = LL, RL, LR, RR$). The covariance matrix \mathcal{C} is the sum of the experimental and theoretical uncertainties, and includes the experimental correlation between $R(D)$ and $R(D^*)$. We will use in our analysis the correlation values -0.38 and -0.47 , from HFLAV [12, 13] and Belle combination [9], respectively.

We first get the minimum of the χ^2 function (χ_{min}^2), and then we use it to assessing the p -value as a measured of goodness-of-fit. The p -value allow us to quantify the level of agreement between the data and the NP scenarios hypothesis [77]. The p -values are obtained as one minus cumulative function distribution for a certain number of degrees of freedom (N_{dof}) [32, 34, 35, 77]. N_{dof} is equal to $N_{\text{dof}} = N_{\text{obs}} - N_{\text{par}}$, where N_{par} is the number of parameters to be fitted. In our analysis we have $N_{\text{obs}} = 6$ for both set of observables S1 and S2. In addition, we also calculate the pull of the SM (pull_{SM}) defined as the p -value corresponding to $\chi_{\text{SM}}^2 - \chi_{\text{min}}^2$, with $\chi_{\text{SM}}^2 = \chi^2(0)$, and converted into an equivalent significance in units of standard deviation (σ) [32, 34, 35, 77].

A. Analysis on the parametric space of the scalar Wilson coefficients

In this analysis we are only interested in two-dimension scenarios regarding scalar WCs. We fit the set of observables S1 and S2 by allowing two scalar WCs different from zero (and setting the others two equal to zero). Depending on the choices for the chiral charges, we have identify three different benchmark scenarios, namely,

1. (C_S^{LL}, C_S^{RL}) : operators with only LH neutrinos,
2. (C_S^{LL}, C_S^{LR}) and (C_S^{LL}, C_S^{RR}) : mixed operators with LH + RH neutrinos,
3. (C_S^{LR}, C_S^{RR}) : operators with only RH neutrinos.

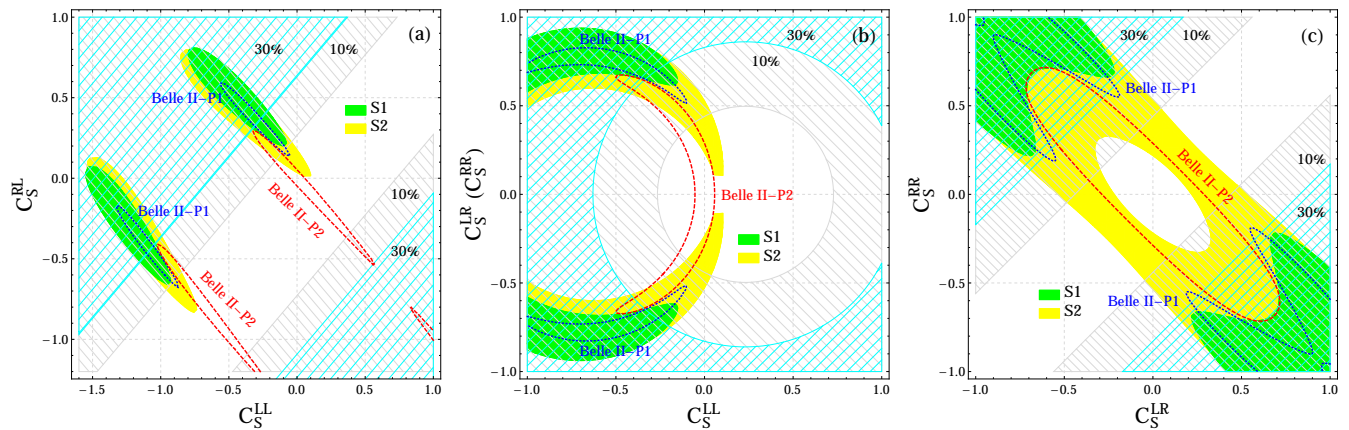


FIG. 1. The 95% C.L. allowed parameter space for the set of observables S1 [green region] and S2 [yellow region] in the planes: (a) (C_S^{LL}, C_S^{RL}) , (b) (C_S^{LL}, C_S^{LR}) or (C_S^{LR}, C_S^{RR}) , and (c) (C_S^{LR}, C_S^{RR}) . The cyan and gray hatched regions represent the excluded regions by the 30% and 10% upper limits on $\text{BR}(B_c^- \rightarrow \tau^- \bar{\nu}_\tau)$, respectively. The projections Belle II-P1 and Belle II-P2 for an integrated luminosity of 50 ab^{-1} are illustrated by the blue dotted and red dashed contour lines, respectively (See the text for details).

In Table II we report our results of the best-fit point (BFP) values, p -value, pull_{SM} , and 1σ allowed intervals. In these two scalar WCs scenarios $N_{\text{par}} = 2$, thus $N_{\text{dof}} = 4$. For the SM we obtained $\chi_{\text{SM}}^2 = 19.1$ (11.2) for the set S1 (S2), corresponding to a $p\text{-value}_{\text{SM}} = 7.6 \times 10^{-4}$ (2.4×10^{-2}). The largest p -value is obtained for the benchmark scenario (C_S^{LL}, C_S^{RL}) , however, scenarios with RH neutrinos have also a favorable p -value. In general, these scenarios provide good quality to adjust the experimental $b \rightarrow c\tau\bar{\nu}_\tau$ anomalies. We have checked that smaller p -values of the order $\sim 24\%$, $\sim 33\%$ and $\sim 18\%$ are obtained for the cases of one, three or four non-zero scalar WCs, respectively, and they do not provide good fits of the data. Furthermore, we show in Table III the Belle II-P1 and Belle II-P2 projections of the 1σ allowed intervals for two scalar WCs scenarios. The Belle II-P1 projection would still allow sizeable couplings, thus, leaving room for significant NP contributions. While for Belle II-P2, these scenarios would be, in general, strongly constrained.

To further discussion, we plot in Fig. 1 the 95% confidence level (C.L.) allowed parameter space in the planes: (a) (C_S^{LL}, C_S^{RL}) , (b) (C_S^{LL}, C_S^{LR}) or (C_S^{LL}, C_S^{RR}) , and (c) (C_S^{LR}, C_S^{RR}) . The green and yellow regions are obtained by considering the set of observables S1 and S2, respectively. The cyan (gray) hatched region shows the disallowed parameter space by $\text{BR}(B_c^- \rightarrow \tau^- \bar{\nu}_\tau) < 30\%$ (10%). The projections Belle II-P1 and Belle II-P2 for an integrated luminosity of 50 ab^{-1} are illustrated by the blue dotted and red dashed contour lines, respectively. The following remarks are obtained:

1. In all of the benchmark two WCs scenarios considered, the allowed regions by the set of observables S1 (dominated by $R(D^{(*)})$ HFLAV) are ruled out by $\text{BR}(B_c^- \rightarrow \tau^- \bar{\nu}_\tau) < 30\%$ and 10% , which is in agreement with the recent analysis of Ref. [29, 32]. Similarly, the available regions from projection Belle II-P1 indicates that these scenarios would be excluded.
2. For the scenario with only LH neutrinos, plane (C_S^{LL}, C_S^{RL}) , it is observed that there are two-fold small allowed regions by the set of observables S2. Moreover, projection Belle II-P2 would leave a small window for NP contributions without violating $\text{BR}(B_c^- \rightarrow \tau^- \bar{\nu}_\tau) < 30\%$ and 10% .
3. As for the scenario LH + RH neutrinos, planes (C_S^{LL}, C_S^{LR}) or (C_S^{LL}, C_S^{RR}) ³, it is also found two-fold small allowed regions by the set of observables S2, and the projection Belle II-P2 would severely constrain the allowed parameter space.
4. Finally, the case with only RH neutrinos, plane (C_S^{LR}, C_S^{RR}) , our findings show two-fold allowed regions by the set S2, that would be reduced by projection Belle II-P2, but still leaving allowed parameter space. Thus, the effective scalar operator with only RH neutrinos offers an interesting solution to the current $b \rightarrow c\tau\bar{\nu}_\tau$ data.

³ Let us notice that the allowed region in the plane (C_S^{LL}, C_S^{LR}) , is the same as in the plane (C_S^{LL}, C_S^{RR}) . This is due to the fact that the scalar WCs, C_S^{LR} and C_S^{RR} , have the same polynomial behavior in all of the observables.

B. Analysis on the parametric space of Yukawa couplings

The previous analysis was made in terms of the scalar WCs involving LH and RH neutrinos. Here, we go a step forward by exploring the implications on the parametric space associated with the charged Higgs Yukawa couplings to the quarks and leptons in the generic 2HDM that can accommodate the charged-current B meson anomalies. In the literature, 2HDMs with a more generic flavor structure have been extensively explored as an explanation to the $R(D^{(*)})$ discrepancies [38–56]. In all these works, the neutrinos have been considered to be LH. Only in Refs. [45, 57, 58], a generic 2HDM involving RH neutrinos has been studied to address the anomalies. In the following, we will study the scenarios for a charged scalar boson with general Yukawa couplings involving LH and RH neutrinos. By “general” we will refer to Yukawa couplings without additional assumptions, such as Cheng-Sher ansatz (see, for instance [49, 50]). In order to provide an explanation to the $b \rightarrow c\tau\bar{\nu}_\tau$ anomalies, we will adopt the phenomenological assumption in which the charged scalar boson (H^\pm) couples only to the bottom-charm quarks and the third generation of leptons τ - ν_τ , i.e., the corresponding Yukawa couplings are different from zero, while the other ones are taken to be zero. Therefore, NP effects are negligible for light lepton modes (e or μ). In addition, we consider these Yukawa couplings as real (charge-parity conserving) arbitrary free parameters.

The most general Lagrangian for the $b \rightarrow c\tau\bar{\nu}_\tau$ transition induced by the Yukawa couplings of a charged scalar boson H^\pm is given by (see Eq. (A12))

$$\begin{aligned} \mathcal{L}_{H^\pm}(b \rightarrow c\tau\bar{\nu}_\tau) = & -H^+ (\bar{c}X_{cb}^D P_R b - \bar{c}X_{bc}^{U*} P_L b + \bar{\nu}_\tau X_{\nu_\tau}^E P_R \tau - \bar{\nu}_\tau X_{\tau\nu_\tau}^{N*} P_L \tau) \\ & -H^- (\bar{b}X_{cb}^{D*} P_L c - \bar{b}X_{bc}^U P_R c + \bar{\tau}X_{\nu_\tau}^{E*} P_L \nu_\tau - \bar{\tau}X_{\tau\nu_\tau}^N P_R \nu_\tau), \end{aligned} \quad (10)$$

where X_{bc}^U , X_{cb}^D , $X_{\nu_\tau}^E$, and $X_{\tau\nu_\tau}^N$ are the Yukawa couplings to the up-quarks, down-quarks, charged leptons and neutrinos, respectively, with $X_{gh}^f = (X_{hg}^f)^*$. We will use the shorthand notation $X_\tau^E \equiv X_{\nu_\tau}^E$ and $X_\tau^N \equiv X_{\tau\nu_\tau}^N$. In particular, we want to emphasize that the fourth and eighth terms in the previous expression correspond to the neutrino Yukawa coupling X_τ^N , which describes the interaction between the RH neutrino and a charged scalar boson. While the third and sixth terms correspond to the charged lepton (electron-like) Yukawa coupling X_τ^E that usually appears for LH neutrinos. In Appendix A, we provide details on the derivation of the Yukawa Lagrangian, Eq. (10), within a general 2HDM with the inclusion of RH neutrinos. To avoid dangerous tree-level flavor-changing neutral currents, we will impose the aligned condition on the down-type quarks [58].

After integrating out H^\pm , the scalar WCs from the effective four-fermion Lagrangian, Eq. (1), are written as (see appendix A1)

$$C_S^{LL} = + \frac{\sqrt{2}}{4G_F V_{cb}^{\text{CKM}}} \frac{(X_{bc}^{U*})(X_\tau^{E*})}{M_{H^\pm}^2}, \quad (11)$$

$$C_S^{RL} = - \frac{\sqrt{2}}{4G_F V_{cb}^{\text{CKM}}} \frac{(X_{cb}^D)(X_\tau^{E*})}{M_{H^\pm}^2}, \quad (12)$$

$$C_S^{LR} = - \frac{\sqrt{2}}{4G_F V_{cb}^{\text{CKM}}} \frac{(X_{bc}^{U*})(X_\tau^N)}{M_{H^\pm}^2}, \quad (13)$$

$$C_S^{RR} = + \frac{\sqrt{2}}{4G_F V_{cb}^{\text{CKM}}} \frac{(X_{cb}^D)(X_\tau^N)}{M_{H^\pm}^2}, \quad (14)$$

with M_{H^\pm} being the H^\pm charged scalar boson mass. Thus, the $b \rightarrow c\tau\bar{\nu}_\tau$ observables, Eqs. (2) to (8), can be expressed in terms of the effective scalar and pseudoscalar contributions, namely

$$C_S^{RL} \pm C_S^{LL} = \frac{\sqrt{2}}{4G_F V_{cb}^{\text{CKM}}} \frac{(\pm X_{bc}^{U*} - X_{cb}^D)(X_\tau^{E*})}{M_{H^\pm}^2}, \quad (15)$$

$$C_S^{LR} \pm C_S^{RR} = \frac{\sqrt{2}}{4G_F V_{cb}^{\text{CKM}}} \frac{(-X_{bc}^{U*} \pm X_{cb}^D)(X_\tau^N)}{M_{H^\pm}^2}, \quad (16)$$

for LH and RH neutrinos, respectively. In the most general case, three Yukawa couplings are always involved in a non trivial way. Keeping this in mind, we perform a χ^2 analysis by allowing three Yukawa couplings different from zero, i.e., $(X_{bc}^U, X_{cb}^D, X_\tau^E)$ for LH neutrinos scenarios and $(X_{bc}^U, X_{cb}^D, X_\tau^N)$ for RH neutrinos scenarios, respectively. We found that simplified scenarios regarding two Yukawa couplings (up- or down-quark and lepton or neutrino) cannot simultaneously accommodate the $R(D)$ and $R(D^*)$ data (even relaxing the uncertainties at the 2σ level) yielding to p -values $\lesssim 8\%$.

We display in Table IV the BFP values, p -value, and pull_{SM} by allowing three Yukawa couplings different from zero to fit the set of observables S1 and S2. Particularly, we observe that the neutrino Yukawa couplings must be

Set S1 ($\chi^2_{\text{SM}} = 19.1$, $p\text{-value}_{\text{SM}} = 7.6 \times 10^{-4}$)			
Yukawa couplings	BFP	$p\text{-value}$ (%)	pull_{SM}
$(X_{bc}^U, X_{cb}^D, X_\tau^E)$	(0.33, 0.38, -0.47)	28.8	2.95
$(X_{bc}^U, X_{cb}^D, X_\tau^N)$	(-0.35, -0.25, -1.09)	28.9	2.95
Set S2 ($\chi^2_{\text{SM}} = 11.2$, $p\text{-value}_{\text{SM}} = 2.4 \times 10^{-2}$)			
Yukawa couplings	BFP	$p\text{-value}$ (%)	pull_{SM}
$(X_{bc}^U, X_{cb}^D, X_\tau^E)$	(0.23, 0.25, -0.64)	28.4	1.56
$(X_{bc}^U, X_{cb}^D, X_\tau^N)$	(-0.38, 0.31, -0.90)	27.7	1.54

TABLE IV. BFP values, p -value, and pull_{SM} by allowing three Yukawa couplings different from zero to fit the set of observables S1 and S2.

as large as one ($|X_\tau^N| \sim 1$) to reproduce the $b \rightarrow c\tau\bar{\nu}_\tau$ data. Furthermore, the 95% C.L. allowed two dimensional parameter space in the Yukawa couplings planes: (a) (X_{bc}^U, X_τ^E) , (b) (X_{cb}^D, X_τ^E) , (c) (X_{bc}^U, X_τ^N) and (d) (X_{cb}^D, X_τ^N) , are shown in Fig. 2. The green and yellow regions represent the allowed parameter space that simultaneously can accommodate the set of observables S1 and S2, respectively. These plots have been obtained for a representative charged Higgs mass of $M_{H^\pm} = 500$ GeV, which corresponds to a benchmark mass value usually considered in the literature [50, 52, 58]. In each case, we vary the Yukawa couplings on the plane while keeping the remaining one at the BFP. The hatched regions in gray and cyan refer to the excluded regions by the 10% and 30% upper limits on $\text{BR}(B_c \rightarrow \tau\bar{\nu}_\tau)$, respectively. The prospects Belle II-P1 and Belle II-P2 for an integrated luminosity of 50 ab^{-1} [26] are illustrated by the blue dotted and red dashed contour lines, respectively. According to our analysis, we get the following remarks:

1. For the Yukawa couplings planes (X_{bc}^U, X_τ^E) and (X_{cb}^D, X_τ^E) related with LH neutrinos, panels 2(a) and 2(b), Yukawa couplings regions with absolute values of the order $\mathcal{O}(10^{-1})$ are allowed by the set of observables S1 and S2, as well as by the prospects Belle II-P1 and Belle II-P2.
2. As concerns with the neutrino Yukawa couplings planes (X_{bc}^U, X_τ^N) and (X_{cb}^D, X_τ^N) (RH neutrino solutions), panels 2(c) and 2(d), both for set of observables S1 and S2 there is a wide allowed region Yukawa couplings with absolute values of the order $\mathcal{O}(10^{-1})$, that would be reduced by the projection Belle II-P2. The case of projection Belle II-P1 would be almost excluded because of bounds $\text{BR}(B_c^- \rightarrow \tau^-\bar{\nu}_\tau) < 30\%$ and 10% . Our results imply that current experimental $b \rightarrow c\tau\bar{\nu}_\tau$ data favors the interpretation of a charged scalar boson with right-handed neutrinos.

IV. DIGGING INTO THE RELATION BETWEEN $R(D^*)$ AND $\text{BR}(B_c^- \rightarrow \tau^-\bar{\nu}_\tau)$

The importance of the relation between $R(D^*)$ and $\text{BR}(B_c^- \rightarrow \tau^-\bar{\nu}_\tau)$ was first pointed out in Ref. [59], where an upper limit of $\text{BR}(B_c^- \rightarrow \tau^-\bar{\nu}_\tau) \leq 30\%$ is imposed by considering the lifetime of B_c meson. This bound puts strong constraints on the pseudoscalar interpretation to $R(D^*)$ generated by the effective coupling $\epsilon_P = C_S^{RL} - C_S^{LL}$ [59]. Later on, a stronger bound of $\text{BR}(B_c^- \rightarrow \tau^-\bar{\nu}_\tau) \leq 10\%$ was obtained in Ref. [60] from the LEP data taken at the Z peak. Recently, these limits have been critically examined and relaxed bounds of $\leq 39\%$ [33] and $\leq 60\%$ [34, 35] have been obtained. In the following, we revisit whether the claim that pseudoscalar NP interpretations of $R(D^*)$ are implausible [59] is still valid (or not) to the light of the recent measurements,

$$\begin{aligned}
R(D^*) &= 0.295 \pm 0.014 \quad \text{HFLAV [12, 13]}, \\
R(D^*) &= 0.284 \pm 0.018 \quad \text{Belle combination [9]}, \\
R(D^*) &= 0.291 \pm 0.035 \quad \text{LHCb [7]},
\end{aligned} \tag{17}$$

by considering $\text{BR}(B_c^- \rightarrow \tau^-\bar{\nu}_\tau) < 30\%$ [59] and 10% [60]. We also include in our analysis the Belle II prospects Belle II-P1 and Belle II-P2 described in Sec. III, to see the future implications that could be achieved at Belle II for an integrated luminosity of 50 ab^{-1} [26].

In Fig. 3 we plot the relation between $R(D^*)$ and $\text{BR}(B_c^- \rightarrow \tau^-\bar{\nu}_\tau)$ for $R(D^*)$ from (a) HFLAV [12, 13], (b) Belle combination [9], (c) LHCb [7], and (d) Belle II prospects Belle II-P1 and Belle II-P1 for 50 ab^{-1} . In all the cases, the band represents the 1σ experimental value. The red solid line shows the parametric dependence of $R(D^*)$ and $\text{BR}(B_c^- \rightarrow \tau^-\bar{\nu}_\tau)$ on the effective coupling ϵ_P , while the dashed and dotted horizontal lines represent the upper limit

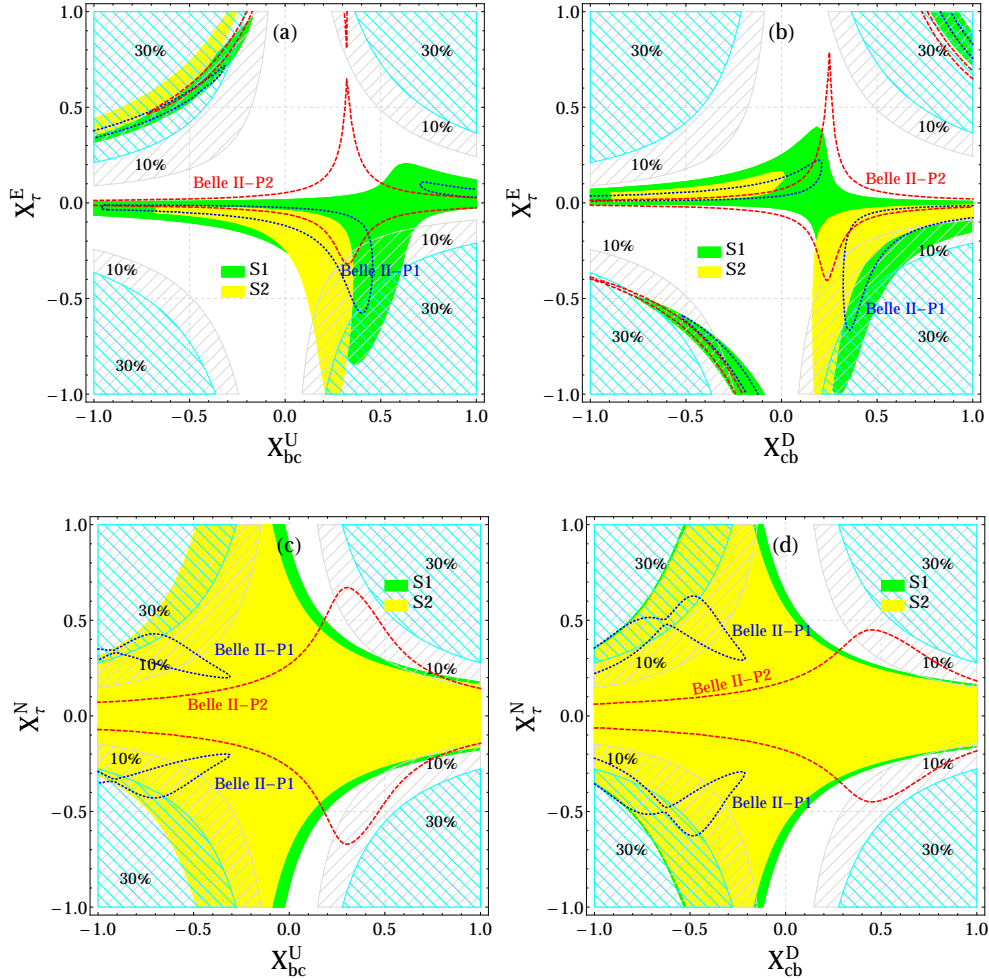


FIG. 2. The 95% C.L. allowed two dimensional parameter space for the sets S1 [green region] and S2 [yellow region] in the Yukawa coupling planes: (a) (X_{bc}^U, X_τ^E) , (b) (X_{bc}^U, X_τ^E) , (c) (X_{cb}^D, X_τ^N) and (d) (X_{cb}^D, X_τ^N) , for a charged Higgs mass of $M_{H^\pm} = 500$ GeV. The hatched regions in gray and cyan represent the excluded regions by the 10% and 30% upper limits on $\text{BR}(B_c^- \rightarrow \tau^- \bar{\nu}_\tau)$, respectively. The projections Belle II-P1 and Belle II-P2 for an integrated luminosity of 50 ab^{-1} [26] are illustrated by the blue dotted and red dashed contour lines, respectively. In each case, we vary the Yukawa couplings on the plane while keeping the remaining one at the BFP.

$\text{BR}(B_c^- \rightarrow \tau^- \bar{\nu}_\tau) < 30\%$ and 10% , respectively. The SM value is represented by the black circle. It is found that the 1σ allowed solutions are

$$\begin{aligned}
 \text{HFLAV} : \epsilon_P &= [0.66, 1.23], \\
 \text{Belle combination} : \epsilon_P &= [0.26, 1.11], \\
 \text{LHCb} : \epsilon_P &= [0.0, 1.53], \\
 \text{Belle II-P1} : \epsilon_P &= [0.58, 0.86], \\
 \text{Belle II-P2} : \epsilon_P &= [0.0, 0.23],
 \end{aligned} \tag{18}$$

respectively, as depicted in Fig. 3. In order to fulfill the bound $\text{BR}(B_c^- \rightarrow \tau^- \bar{\nu}_\tau) < 30\%$ (10%), the maximum value required is $\epsilon_P^{\text{max}} = 0.63$ (0.26), corresponding to a value of $R(D^*) = 0.281$ (0.266). For the case of HFLAV, the allowed ϵ_P values violate the bound $\text{BR}(B_c^- \rightarrow \tau^- \bar{\nu}_\tau) < 30\%$. In contrast, the allowed ϵ_P values for Belle combination satisfy both $\text{BR}(B_c^- \rightarrow \tau^- \bar{\nu}_\tau) < 30\%$ and 10% . On the other hand, the experimental uncertainties of the LHCb data are large enough to be consistent with the bounds $\text{BR}(B_c^- \rightarrow \tau^- \bar{\nu}_\tau) < 30\%$ and 10% , as well as with the SM. As for the Belle II-P1 would only respect the limit of 30% , while for Belle II-P2, small values of ϵ_P would be favored in fulfillment with the limits of 30% and 10% . In addition, Belle II-P2 would also be able to prove an aggressive bound of $\text{BR}(B_c^- \rightarrow \tau^- \bar{\nu}_\tau) < 5\%$.

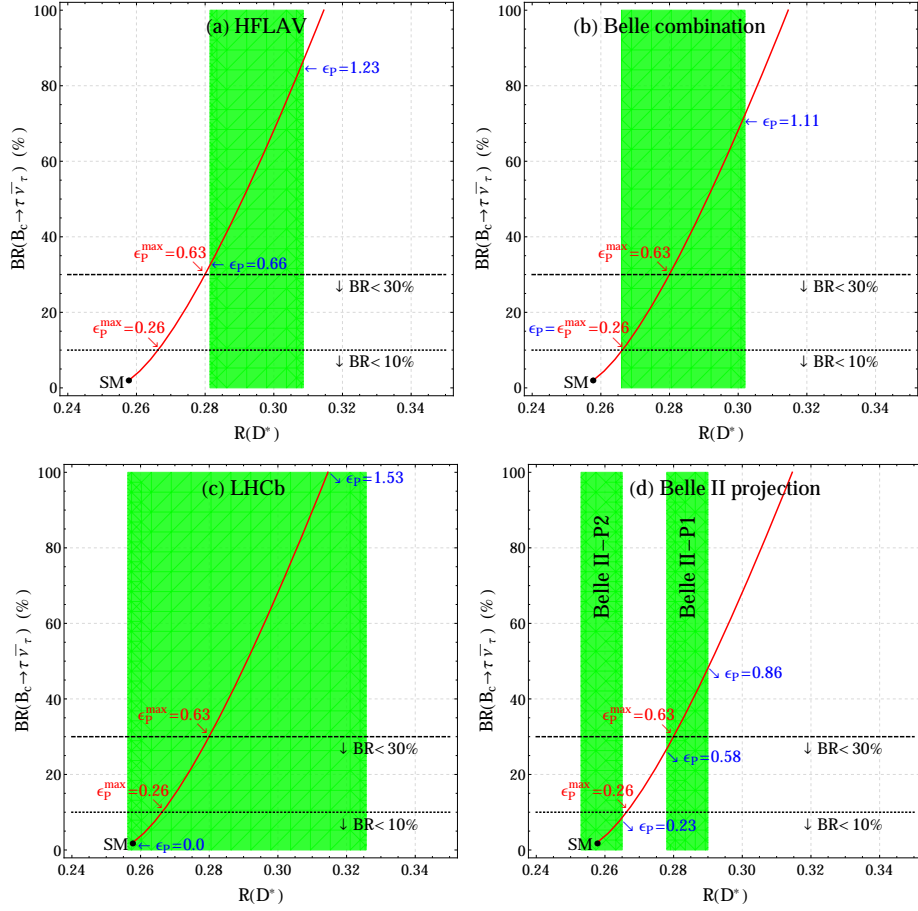


FIG. 3. Relation between $R(D^*)$ and $\text{BR}(B_c^- \rightarrow \tau^- \bar{\nu}_\tau)$ for $R(D^*)$ from (a) HFLAV [12, 13], (b) Belle combination [9], (c) LHCb [7], and (d) Belle II prospects Belle II-P1 and Belle II-P2; represented by the green 1σ band, respectively. The red solid line shows the parametric dependence of $R(D^*)$ and $\text{BR}(B_c^- \rightarrow \tau^- \bar{\nu}_\tau)$ on the effective coupling ϵ_P . The dashed (dotted) horizontal line represents $\text{BR}(B_c^- \rightarrow \tau^- \bar{\nu}_\tau) < 30\%$ (10%).

Therefore, $\text{BR}(B_c^- \rightarrow \tau^- \bar{\nu}_\tau) < 30\%$ [59] still disfavors the ϵ_P pseudoscalar explanation of the $R(D^*)$ HFLAV average, while this is no longer the case for the $R(D^*)$ data from Belle combination [9] and LHCb [7]. The projection Belle II-P1 would not be in conflict with $\text{BR}(B_c^- \rightarrow \tau^- \bar{\nu}_\tau) < 30\%$, whereas the projection Belle II-P2 would lead to stronger constraints than those obtained from $\text{BR}(B_c^- \rightarrow \tau^- \bar{\nu}_\tau)$. Certainly, future measurements by the Belle II [26] (as well as LHCb) experiment are required in order to clarify this situation.

V. REEXAMINING THE EXPLANATION FROM 2HDM OF TYPE II

The 2HDM of Type II provides one of the simplest scenarios with charged scalar bosons (H^\pm). Within this framework, the NP effects of a charged Higgs boson depend on the mass of charged scalar boson M_{H^\pm} and $\tan\beta$ (defined as the ratio of vacuum expectation values v_2/v_1), which are described in terms of a single parameter, $\tan\beta/M_{H^\pm}$. In the 2HDM of Type II, tree-level charged Higgs boson contributions to the B meson processes induced by the semileptonic transition $b \rightarrow c\tau\bar{\nu}_\tau$ have been investigated (See, for instance [78–83]). In 2012 and 2013, the BABAR Collaboration with their full data sample reported a disagreement on the measurements of the ratio of semileptonic B decays, $R(D)$ and $R(D^*)$, with respect to the SM predictions [1, 2]. According to the BABAR results, the 2HDM of Type II cannot explain simultaneously the $R(D^{(*)})$ discrepancies [1, 2]. Since then (and to date), the 2HDM of Type II interpretation was ruled out and 2HDM models with a more generic flavor structure were considered in the literature [38–58]. It is worth noting that subsequent analysis performed by Belle Collaboration in 2015 [3] and 2016 [4] showed compatibility with the 2HDM of Type II in the $\tan\beta/M_{H^\pm}$ regions around 0.45 GeV^{-1} [3] and $[0.65, 0.76] \text{ GeV}^{-1}$ [4], respectively, in contradiction with the BABAR measurements [1, 2]. Thereby, given the current experimental situation on the $R(D^{(*)})$ anomalies, HFLAV [12, 13] and Belle combination [9], and the Belle II future sensitivity [26], in this section

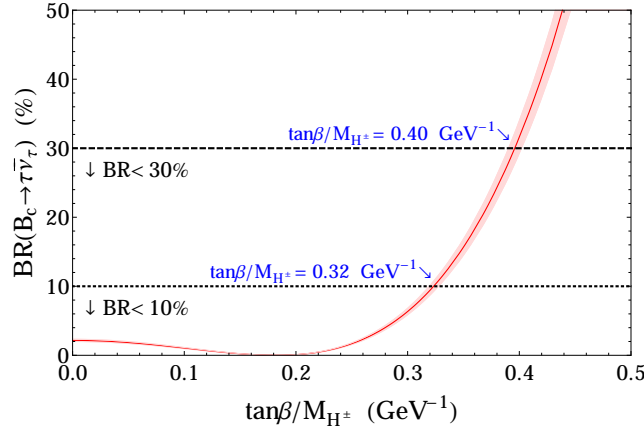


FIG. 4. $\text{BR}(B_c^- \rightarrow \tau^- \bar{\nu}_\tau)$ in the 2HDM of type II as a function of $\tan \beta / M_{H^\pm}$ (red solid line). The light-red band represents the 1σ error, while the dashed and dotted horizontal lines represent $\text{BR}(B_c^- \rightarrow \tau^- \bar{\nu}_\tau) < 30\%$ and 10% , respectively.

we reexamine whether the 2HDM of Type II is still ruled out (or not) as an explanation to the $R(D^{(*)})$ anomalies. In addition, it is also important to confront this model not only to the $R(D^{(*)})$ measurements but also to all $b \rightarrow c\tau\bar{\nu}_\tau$ observables.

By construction, in the 2HDM of Type II the neutrinos are considered to be LH, therefore, the scalar WCs that contribute to the charged-current $b \rightarrow c\tau\bar{\nu}_\tau$ are written as [4, 17, 79]

$$C_S^{RL} = -\frac{m_b m_\tau \tan \beta}{M_{H^\pm}^2}, \quad (19)$$

$$C_S^{LL} = -\frac{m_c m_\tau}{M_{H^\pm}^2}, \quad (20)$$

where m_b , m_c , and m_τ are the masses of the bottom quark, charm quark, and τ lepton, respectively. In the literature [4, 17, 79], the coefficient C_S^{LL} is usually neglected ($C_S^{LL} \simeq 0$), thus, the charged Higgs boson effect is only dominated by C_S^{RL} which is driven by $\tan \beta / M_{H^\pm}$. We begin our analysis by considering the constraints on the parameter $\tan \beta / M_{H^\pm}$ from the upper limits $\text{BR}(B_c^- \rightarrow \tau^- \bar{\nu}_\tau) < 30\%$ [59] and 10% [60]. In Fig. 4 we show the $\text{BR}(B_c^- \rightarrow \tau^- \bar{\nu}_\tau)$ in the 2HDM of type II as a function of $\tan \beta / M_{H^\pm}$ (red solid line), where the dashed and dotted horizontal lines represent $\text{BR}(B_c^- \rightarrow \tau^- \bar{\nu}_\tau) < 30\%$ and 10% , respectively. We get the following strong bounds

$$\tan \beta / M_{H^\pm} < 0.40 \quad (0.32), \quad (21)$$

for $\text{BR}(B_c^- \rightarrow \tau^- \bar{\nu}_\tau) < 30\%$ (10%), implying that large values of $\tan \beta / M_{H^\pm}$ are excluded. This plot has been obtained by using the SM estimation $\text{BR}(B_c^- \rightarrow \tau^- \bar{\nu}_\tau)_{\text{SM}} = (2.16 \pm 0.16)\%$ [71]. In addition, in Table V we present the 2σ allowed regions by each of the $b \rightarrow c\tau\bar{\nu}_\tau$ observables on the parameter $\tan \beta / M_{H^\pm}$, namely, $R(D^{(*)})$ HFLAV and Belle combination, $R(J/\psi)$, $F_L(D^*)$, $P_\tau(D^*)$, and $R(X_c)$. Regarding the Belle II future scenario described in Sec. III, we also show the prospects Belle II-P1 and Belle II-P2 that could be achieved at Belle II for an integrated luminosity of 50 ab^{-1} [26]. As a result, it is possible to find a common small values region, $\tan \beta / M_{H^\pm} = [0.0, 0.32]$, without conflicting with the strongest bound imposed by $\text{BR}(B_c^- \rightarrow \tau^- \bar{\nu}_\tau) < 10\%$; with the exception of $R(D^{(*)})$ HFLAV and $R(J/\psi)$ that allows large $\tan \beta / M_{H^\pm}$ values, which are in tension with $\text{BR}(B_c^- \rightarrow \tau^- \bar{\nu}_\tau) < 30\%$ and 10% . Besides, the projected Belle II-P1 values would be rule out by the bounds of 30% and 10% , while the projection Belle II-P2 would point out to small values of $\tan \beta / M_{H^\pm}$.

To further discussion, we now translate these results into the plane $(M_{H^\pm}, \tan \beta)$ of the 2HDM of Type II, as is shown in Figs. 5(a) and 5(b) by the gray region for the $R(D^{(*)})$ solutions from Belle combined and Belle II 50 ab^{-1} , respectively. The red hatched region corresponds to the 95% C.L. strong bound on the charged Higgs mass $M_{H^\pm} > 580 \text{ GeV}$ (independent of $\tan \beta$), obtained from inclusive radiative decays of the B meson, $B \rightarrow X_{s,d}\gamma$ [84]. In addition, we also considered the tree-level contributions from the charged Higgs boson exchange in the tauonic decay $B \rightarrow \tau\bar{\nu}_\tau$ [80]

$$\text{BR}(B^- \rightarrow \tau^- \bar{\nu}_\tau) = \text{BR}(B^- \rightarrow \tau^- \bar{\nu}_\tau)_{\text{SM}} \left(1 - \tan^2 \beta \frac{m_B^2}{M_{H^\pm}^2}\right)^2. \quad (22)$$

Observable	Allowed regions (2σ) on $\tan\beta/M_{H^\pm}$ (GeV^{-1})
$R(D)$ HFLAV	$[0.0, 0.08] \cup [0.44, 0.47]$
$R(D)$ Belle combination	$[0.0, 0.11] \cup [0.43, 0.47]$
$R(D)$ Belle II-P1	$[0.45, 0.46]$
$R(D)$ Belle II-P2	$[0.0, 0.06] \cup [0.44, 0.45]$
$R(D^*)$ HFLAV	$[0.64, 0.75]$
$R(D^*)$ Belle combination	$[0.0, 0.24] \cup [0.56, 0.75]$
$R(D^*)$ Belle II-P1	$[0.67, 0.70]$
$R(D^*)$ Belle II-P2	$[0.0, 0.17] \cup [0.58, 0.63]$
$R(J/\psi)$	$[1.0, 1.05]$
$F_L(D^*)$	$[0.0, 0.09] \cup [0.44, 0.67]$
$P_\tau(D^*)$	$[0.0, 0.32] \cup [0.56, 1.03]$
$R(X_c)$	$[0.0, 0.17] \cup [0.44, 0.72]$

TABLE V. The 2σ allowed regions on the parameter $\tan\beta/M_{H^\pm}$ of the 2HDM of Type II, obtained for the different $b \rightarrow c\tau\bar{\nu}_\tau$ observables. The Belle II future projections for an integrated luminosity of 50 ab^{-1} are also included.

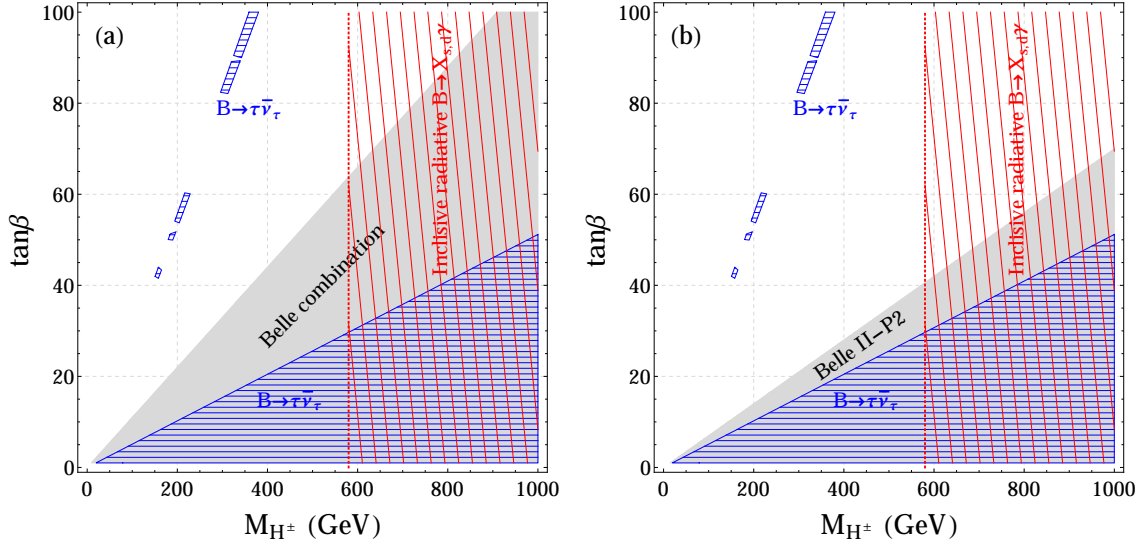


FIG. 5. Allowed parameter space in the plane $(M_{H^\pm}, \tan\beta)$ of the 2HDM Type II for (a) Belle combination and (b) Belle II-P2 for 50 ab^{-1} . The allowed regions by $B \rightarrow \tau\bar{\nu}_\tau$ and the inclusive radiative decays $B \rightarrow X_{s,d}\gamma$ [84] are represented by the blue and red hatched regions, respectively.

with

$$\text{BR}(B^- \rightarrow \tau^- \bar{\nu}_\tau)_{\text{SM}} = \tau_B \frac{G_F^2}{8\pi} |V_{ub}|^2 f_B^2 m_B m_\tau^2 \left(1 - \frac{m_\tau^2}{m_B^2}\right)^2, \quad (23)$$

where V_{ub} denotes the CKM matrix element involved, and f_B and τ_B are the B^- meson decay constant and lifetime, respectively. By using $f_B = (190.0 \pm 1.3) \text{ MeV}$ and $V_{ub} = (3.94 \pm 0.36) \times 10^{-3}$ from Particle Data Group (PDG) [77], we get a SM prediction of $\text{BR}(B^- \rightarrow \tau^- \bar{\nu}_\tau)_{\text{SM}} = (9.89 \pm 0.13) \times 10^{-5}$ that is in agreement (0.4σ) with the experimental value $\text{BR}(B^- \rightarrow \tau^- \bar{\nu}_\tau)_{\text{Exp}} = (10.9 \pm 2.4) \times 10^{-5}$ reported by PDG [77]. The allowed regions from $B \rightarrow \tau\bar{\nu}_\tau$ are represented by the blue hatched regions in Figs. 5(a) and 5(b). For the Belle combination we found that for $30 \lesssim \tan\beta \lesssim 70$, it is possible to get a large region on the parameter space $(M_{H^\pm}, \tan\beta)$ to account for a joint explanation to the $R(D)$ and $R(D^*)$ anomalies, in consistency with $B \rightarrow \tau\bar{\nu}_\tau$ and bounds from inclusive radiative B decays ($M_{H^\pm} > 580 \text{ GeV}$). On the other hand, the projection Belle II-P2 suggests that the 2HDM of Type II would be no longer disfavored.

VI. SUMMARY AND CONCLUSIONS

Given the present-day 2020 experimental $b \rightarrow c\tau\bar{\nu}_\tau$ data, we analysed the so-called charged-current B meson anomalies in terms of a charged scalar boson within the framework of a generic 2HDM. We performed a model independent analysis based on the most general effective Hamiltonian with all the four-fermion scalar operators involving LH and RH neutrinos. We first explored the associated scalar WCs by paying special attention to those including RH neutrinos, namely C_S^{LR} and C_S^{RR} . Our study is composed of two set of observables that include the HFLAV world-average and Belle combination measurements on $R(D^{(*)})$, along with $R(J/\psi)$, the polarizations $P_\tau(D^*)$ and $F_L(D^*)$, the inclusive ratio $R(X_c)$, as well as taking into account the upper limits $\text{BR}(B_c^- \rightarrow \tau^- \bar{\nu}_\tau) < 30\%$ and 10% [59, 60]. We have also investigated the impact of future measurements at Belle II for $R(D^{(*)})$, by regarding two well-motivated projected scenarios that could be achieved for an integrated luminosity of 50 ab^{-1} (referred by us as Belle II-P1 and Belle II-P2). Our results show that there is an allowed region in the parametric space (C_S^{LR}, C_S^{RR}) , even for the projection Belle II-P2. Therefore, the effective scalar operators with RH neutrinos offers an interesting solution to the $b \rightarrow c\tau\bar{\nu}_\tau$ anomalies.

In the second part of our analysis, we go a step forward by exploring the implications of scenarios for a general charged scalar boson with Yukawa couplings involving LH and RH neutrinos. We presented a phenomenological study of the parameter space associated with the charged Higgs Yukawa couplings to the charm-bottom and leptons from third generation in the generic 2HDM that can accommodate the charged-current B meson anomalies. By focusing on RH neutrino scenarios, it is found that for parameter spaces with neutrino Yukawa couplings, there are allowed regions with absolute values of the Yukawa couplings of the order $\mathcal{O}(10^{-1})$, for a benchmark charged Higgs mass of $M_{H^\pm} = 500 \text{ GeV}$. Again, these results imply that current experimental $b \rightarrow c\tau\bar{\nu}_\tau$ data favors the interpretation of a charged scalar boson with RH neutrinos.

As an important by product of our analysis regarding the charged scalar boson explanation, we revisited whether the claim that pseudoscalar NP (ϵ_P) interpretations of $R(D^*)$ are implausible due to the B_c lifetime [59], is still valid to the light of the recent $R(D^*)$ measurements. We found that $\text{BR}(B_c^- \rightarrow \tau^- \bar{\nu}_\tau) < 30\%$ still disfavors the ϵ_P pseudoscalar explanation of the $R(D^*)$ HFLAV average value, while this is no longer the case for the $R(D^*)$ data from Belle combination [9] and LHCb [7]. The projections Belle II-P1 and Belle II-P2 would not be in conflict with $\text{BR}(B_c^- \rightarrow \tau^- \bar{\nu}_\tau) < 30\%$. Future measurements at Belle II experiment are required in order to clarify this situation.

Finally, we also reexamined whether the 2HDM of Type II is still disfavored as an explanation to the $R(D^{(*)})$ anomalies. As the main outcome from this analysis, it is found that for Belle combination is possible to get a large region on the parameter space $(M_{H^\pm}, \tan\beta)$ to account for a joint explanation to the $R(D)$ and $R(D^*)$ anomalies, in consistency with $B \rightarrow \tau\bar{\nu}_\tau$ and bounds from inclusive radiative B decays ($M_{H^\pm} > 580 \text{ GeV}$). This allowed parameter space is not in conflict with the strong bounds $\tan\beta/M_{H^\pm} < 0.40$ and 0.32 that can be set from $\text{BR}(B_c^- \rightarrow \tau^- \bar{\nu}_\tau) < 30\%$ and 10% , respectively, implying that large values of $\tan\beta/M_{H^\pm}$ are excluded. Moreover, the projection Belle II-P2 point out that this model would be no longer disfavored. Thus, after almost eight years, there are good prospects that the 2HDM of Type II explanation will rise from the ashes.

ACKNOWLEDGMENTS

J. Cardozo and J. H. Muñoz are grateful with the Oficina de Investigaciones - Universidad del Tolima by financial support. N. Quintero acknowledges support from Dirección General de Investigaciones - Universidad Santiago de Cali under Project No. 935-621120-G01. E. Rojas acknowledges support from “Vicerrectoría de Investigaciones e Interacción Social VIIS de la Universidad de Nariño”, project numbers 1928 and 2172.

Appendix A: General two Higgs doublet model

The most general Lagrangian for the interaction of two Higgs doublets Φ_1, Φ_2 with the fermions of the SM is given by

$$\begin{aligned} \mathcal{L} &= -\bar{q}_L^i \Phi_1 y_{ij}^{1D} d_R^j - \bar{q}_L^i \Phi_2 y_{ij}^{2D} d_R^j - \bar{q}_L^i \tilde{\Phi}_1 y_{ij}^{1U} u_R^j - \bar{q}_L^i \tilde{\Phi}_2 y_{ij}^{2U} u_R^j \\ &\quad - \bar{l}_L^i \Phi_1 y_{ij}^{1E} e_R^j - \bar{l}_L^i \Phi_2 y_{ij}^{2E} e_R^j - \bar{l}_L^i \tilde{\Phi}_1 y_{ij}^{1N} \nu_R^j - \bar{l}_L^i \tilde{\Phi}_2 y_{ij}^{2N} \nu_R^j \\ &= -\bar{q}_L^i \Phi_\alpha y_{ij}^{\alpha D} d_R^j - \bar{q}_L^i \tilde{\Phi}_\alpha y_{ij}^{\alpha U} u_R^j - \bar{l}_L^i \Phi_\alpha y_{ij}^{\alpha E} e_R^j - \bar{l}_L^i \tilde{\Phi}_\alpha y_{ij}^{\alpha N} \nu_R^j, \end{aligned} \quad (\text{A1})$$

where a sum is assumed on repeated indices. Here i, j run over 1, 2, 3 and α over 1, 2. The super index U refers to up-like quarks (the same is true for the super indices D, E, N which refer to down-like, electron-like, neutrino-like

fermions, respectively). The Higgs boson doublet fields are parametrized as follows:

$$\Phi_\alpha = \begin{pmatrix} \phi_\alpha^+ \\ \frac{v_\alpha + \phi_\alpha^0 + iG_\alpha^0}{\sqrt{2}} \end{pmatrix}, \quad \tilde{\Phi}_\alpha = i\sigma_2 \Phi_\alpha^*. \quad (\text{A2})$$

It is necessary to rotate to the Georgi basis, i.e.,

$$\begin{pmatrix} H_1 \\ H_2 \end{pmatrix} = \begin{pmatrix} \cos \beta & \sin \beta \\ -\sin \beta & \cos \beta \end{pmatrix} \begin{pmatrix} \Phi_1 \\ \Phi_2 \end{pmatrix} \equiv R_{\beta\alpha} \Phi_\alpha, \quad (\text{A3})$$

where $\tan \beta = \frac{v_2}{v_1}$. This basis is chosen in such a way that only the neutral component of H_1 acquires a vacuum expectation value $v/\sqrt{2}$ with $v = \sqrt{v_1^2 + v_2^2}$. In this way $\Phi_\alpha y_{ij}^{\alpha F} = y_{ij}^{\alpha F} (R_{\alpha\beta}^T) R_{\beta\gamma} \Phi_\gamma = \mathcal{Y}_{ij}^{\beta F} H_\beta$. Where we have defined

$$H_\beta = R_{\beta\alpha} \Phi_\alpha, \quad \text{and} \quad \mathcal{Y}_{ij}^{\beta F} = R_{\beta\alpha} y_{ij}^{\alpha F}. \quad (\text{A4})$$

$$(\text{A5})$$

By writing $\mathcal{Y}_{ij}^{\alpha F}$ explicitly we can classify the different Two Higgs Doublet Model (2HDM) types

$$\begin{aligned} \mathcal{Y}_{ij}^{1F} &= +\cos \beta y_{i,j}^{1F} + \sin \beta y_{i,j}^{2F} \\ \mathcal{Y}_{ij}^{2F} &= -\sin \beta y_{i,j}^{1F} + \cos \beta y_{i,j}^{2F}. \end{aligned} \quad (\text{A6})$$

With these definitions equation (A1) becomes

$$\mathcal{L} = -\bar{q}_L^i H_\beta \mathcal{Y}_{ij}^{\beta D} d_R^j - \bar{q}_L^i \tilde{H}_\beta \mathcal{Y}_{ij}^{\beta U} u_R^j - \bar{l}_L^i H_\beta \mathcal{Y}_{ij}^{\beta E} e_R^j - \bar{l}_L^i \tilde{H}_\beta \mathcal{Y}_{ij}^{\beta N} \nu_R^j. \quad (\text{A7})$$

It is necessary to rotate to the mass eigenstates of the fermion mass, i.e.,

$$f_{L,R} = U_{L,R}^F f'_{L,R}. \quad (\text{A8})$$

From the Lagrangian for the charged currents

$$\begin{aligned} \mathcal{L}_{CC} &= -\frac{g}{\sqrt{2}} \bar{u}'_{Li} \gamma^\mu d'_{Li} W^+ - \frac{g}{\sqrt{2}} \bar{e}'_{Li} \gamma^\mu \nu'_{Li} W^- + \text{h.c.} \\ &= -\frac{g}{\sqrt{2}} \bar{u}_{Li} \gamma^\mu V_{CKM} d_{Li} W^+ - \frac{g}{\sqrt{2}} \bar{e}_{Li} \gamma^\mu V_{PMNS} \nu_{Li} W^- + \text{h.c.}, \end{aligned} \quad (\text{A9})$$

it is possible to obtain the Cabibbo-Kobayashi-Maskawa (CKM) and the Pontecorvo-Maki-Nakagawa-Sakata (PMNS) mixing matrices $V_{CKM} = U_L^U U_L^{D\dagger}$ and $V_{PMNS} = U_L^E U_L^{N\dagger}$ by rotating to the fermion mass eigenstates to obtain an expression for the Yukawa couplings closely related to the observables and the Wilson coefficients

$$\mathcal{L}_{H^\pm} = -\bar{u}'_{Li} H_\beta^+ \mathcal{Y}_{ij}^{\beta D} d_R^j + \bar{d}'_{Li} H_\beta^+ \mathcal{Y}_{ij}^{\beta U} u_R^j - \bar{\nu}'_{Li} H_\beta^+ \mathcal{Y}_{ij}^{\beta E} e_R^j + \bar{e}'_{Li} H_\beta^+ \mathcal{Y}_{ij}^{\beta N} \nu_R^j + \text{h.c.} \quad (\text{A10})$$

The charged Higgs fields H_1^\pm are absorbed by the W^\pm bosons in such a way the unique charged scalars are H_2^\pm , which from now on we will simply denote as H^\pm

$$\begin{aligned} \mathcal{L}(H^\pm) &= -H^+ (\bar{u}_L^h X_{u^h d^k}^D d_R^k - \bar{u}_R^h X_{d^h u^k}^{U*} d_L^k + \bar{\nu}_L^h X_{\nu^h e^k}^E e_R^k - \bar{\nu}_R^h X_{e^h \nu^k}^{N*} e_L^k) \\ &\quad - H^- (\bar{d}_R^h X_{u^h d^k}^{D*} u_L^k + \bar{e}_R^h X_{\nu^h e^k}^{E*} \nu_L^k - \bar{d}_L^h X_{d^h u^k}^U u_R^k - \bar{e}_L^h X_{e^h \nu^k}^N \nu_R^k). \end{aligned} \quad (\text{A11})$$

Where $X_{n^h p^k}^P = \left(U_L^N \mathcal{Y}^{2P} U_R^{P\dagger} \right)^{hk}$ and $X_{p^h n^k}^N = \left(U_L^P \mathcal{Y}^{2N} U_R^{N\dagger} \right)^{hk}$, here we label the up and down isospin components with P and N , respectively. The corresponding couplings for the boson H_1 are denoted by $Y_{n^h p^k}^P$ and $Y_{p^h n^k}^N$. We are interested in beyond the SM contributions to the effective Lagrangian, which can explain the charged current anomalies, i.e.,

$$\begin{aligned} \mathcal{L}_{H^\pm}(b \rightarrow c\tau \bar{\nu}_\tau) &= -H^+ (\bar{c} X_{cb}^D P_R b - \bar{c} X_{bc}^{U*} P_L b + \bar{\nu} X_{\nu\tau}^E P_R \tau - \bar{\nu} X_{\tau\nu}^{N*} P_L \tau) \\ &\quad - H^- (\bar{b} X_{cb}^{D*} P_L c - \bar{b} X_{bc}^U P_R c + \bar{\tau} X_{\nu\tau}^{E*} P_L \nu - \bar{\tau} X_{\tau\nu}^N P_R \nu). \end{aligned} \quad (\text{A12})$$

	C_S^{LL}	C_S^{RL}
I	$+V_{PMNS}^{\nu\tau} \frac{m_c m_\tau}{M_{H^\pm}^2} \cot^2 \beta$	$-V_{PMNS}^{\tau\nu} \frac{m_b m_\tau}{M_{H^\pm}^2} \cot^2 \beta$
II	$-V_{PMNS}^{\tau\nu} \frac{m_c m_\tau}{M_{H^\pm}^2}$	$-V_{PMNS}^{\tau\nu} \frac{m_b m_\tau}{M_{H^\pm}^2} \tan^2 \beta$
X	$-V_{PMNS}^{\tau\nu} \frac{m_c m_\tau}{M_{H^\pm}^2}$	$+V_{PMNS}^{\tau\nu} \frac{m_b m_\tau}{M_{H^\pm}^2}$
Y	$+V_{PMNS}^{\tau\nu} \frac{m_c m_\tau}{M_{H^\pm}^2} \cot^2 \beta$	$+V_{PMNS}^{\tau\nu} \frac{m_b m_\tau}{M_{H^\pm}^2}$

TABLE VI. Wilson coefficients for several 2HDMs in the literature. For a precise definition of these models see appendix A 2.

1. Effective Lagrangian

Since the quark level the process $\bar{B} \rightarrow D^{(*)} \tau^- \bar{\nu}_\tau$ is given by $b \rightarrow c \tau^- \bar{\nu}_\tau$, it can be mediated, at tree level, by the additional Higgs H^- with the following Feynman rules

$$\begin{aligned}
b_R &\longrightarrow c_L, H^-, & -iX_{cb}^D \\
b_L &\longrightarrow c_R, H^-, & +iX_{bc}^{U*} \\
H^- &\longrightarrow \tau_R^-, \bar{\nu}_{\tau L}, & -iX_{\nu\tau}^{E*} \\
H^- &\longrightarrow \tau_L^-, \bar{\nu}_{\tau R}, & +iX_{\tau\nu}^N.
\end{aligned} \tag{A13}$$

The process $b \rightarrow c \tau^- \bar{\nu}_\tau$ can be realized in four different ways

$$\begin{aligned}
b_R \rightarrow c_L, H^- (\rightarrow \tau_R^-, \bar{\nu}_{\tau L}), & \quad i\mathcal{L}_1 = \bar{c}_L (-iX_{cb}^D) b_R \frac{i}{M_{H^\pm}^2} \bar{\tau}_R (-iX_{\nu\tau}^{E*}) \nu_L^{(+)} \\
b_R \rightarrow c_L, H^- (\rightarrow \tau_L^-, \bar{\nu}_{\tau R}), & \quad i\mathcal{L}_2 = \bar{c}_L (-iX_{cb}^D) b_R \frac{i}{M_{H^\pm}^2} \bar{\tau}_L (+iX_{\tau\nu}^N) \nu_R^{(+)} \\
b_L \rightarrow c_R, H^- (\rightarrow \tau_R^-, \bar{\nu}_{\tau L}), & \quad i\mathcal{L}_3 = \bar{c}_R (+iX_{bc}^{U*}) b_L \frac{i}{M_{H^\pm}^2} \bar{\tau}_R (-iX_{\nu\tau}^{E*}) \nu_L^{(+)} \\
b_L \rightarrow c_R, H^- (\rightarrow \tau_L^-, \bar{\nu}_{\tau R}), & \quad i\mathcal{L}_4 = \bar{c}_R (+iX_{bc}^{U*}) b_L \frac{i}{M_{H^\pm}^2} \bar{\tau}_L (+iX_{\tau\nu}^N) \nu_R^{(+)}.
\end{aligned} \tag{A14}$$

Thus, the effective Lagrangian for $b \rightarrow c \tau^- \bar{\nu}_\tau$ transition is written as

$$\begin{aligned}
\mathcal{L}_{\text{eff}}^{H^\pm} (b \rightarrow c \tau \bar{\nu}_\tau) &= \frac{4G_F}{\sqrt{2}} V_{cb}^{\text{CKM}} \left[C_S^{LL} (\bar{c} P_L b) (\bar{\tau} P_L \nu_\tau) + C_S^{RL} (\bar{c} P_R b) (\bar{\tau} P_L \nu_\tau) \right. \\
&\quad \left. + C_S^{LR} (\bar{c} P_L b) (\bar{\tau} P_R \nu_\tau) + C_S^{RR} (\bar{c} P_R b) (\bar{\tau} P_R \nu_\tau) \right],
\end{aligned} \tag{A15}$$

where

$$C_S^{LL} = + \frac{\sqrt{2}}{4G_F V_{cb}^{\text{CKM}}} \frac{(X_{bc}^{U*}) (X_{\nu\tau}^{E*})}{M_{H^\pm}^2}, \tag{A16}$$

$$C_S^{RL} = - \frac{\sqrt{2}}{4G_F V_{cb}^{\text{CKM}}} \frac{(X_{cb}^D) (X_{\nu\tau}^{E*})}{M_{H^\pm}^2}, \tag{A17}$$

$$C_S^{LR} = - \frac{\sqrt{2}}{4G_F V_{cb}^{\text{CKM}}} \frac{(X_{bc}^{U*}) (X_{\tau\nu}^N)}{M_{H^\pm}^2}, \tag{A18}$$

$$C_S^{RR} = + \frac{\sqrt{2}}{4G_F V_{cb}^{\text{CKM}}} \frac{(X_{cb}^D) (X_{\tau\nu}^N)}{M_{H^\pm}^2}. \tag{A19}$$

We can obtain explicit expressions for these coefficients with the results of the appendix A 4

2. Couplings for the 2HDMs

From the equation (A6) we have the following expressions for the couplings

$$\begin{aligned} Y_{g^h f^k}^F &= \left(U_L^G \mathcal{Y}^{1F} U_R^{F\dagger} \right)^{hk} = \left(U_L^G [+ \cos \beta y^{1F} + \sin \beta y^{2F}] U_R^{F\dagger} \right)^{hk} \\ X_{g^h f^k}^F &= \left(U_L^G \mathcal{Y}^{2F} U_R^{F\dagger} \right)^{hk} = \left(U_L^G [- \sin \beta y^{1F} + \cos \beta y^{2F}] U_R^{F\dagger} \right)^{hk}. \end{aligned} \quad (\text{A20})$$

In these expressions g and f run over the Yukawa matrices superscripts u, d, e and ν in such a way that for a charged Higgs $(g^h, h^k, F) \in \{(u^h, d^k, D), (d^h, u^k, U), (\nu^h, e^k, N), (e^h, \nu^k, E)\}$. From these definitions the following 2HDM types are well known in the literature

- Type I: all masses of quarks and leptons are given by Φ_2 , i.e., $y_{ij}^{1D} = y_{ij}^{1U} = y_{ij}^{1E} = 0$.
- Type II: the up-type quarks obtain their masses from Φ_2 , while the down-type quarks and charged leptons from Φ_1 , i.e., $y_{ij}^{2D} = y_{ij}^{1U} = y_{ij}^{2E} = 0$.
- Type X: the quarks obtain their masses from Φ_2 , and the leptons from Φ_1 , i.e., $y_{ij}^{1D} = y_{ij}^{1U} = y^{2E} : ij = 0$
- Type Y: the down-like quarks obtain their masses from Φ_1 and the remaining SM fermions acquire their masses from Φ_2 , i.e., $y_{ij}^{2D} = y_{ij}^{1U} = y_{ij}^{1E} = 0$.

As we will see later these models avoid flavor changing neutral currents (FCNC), which it is quite convenient for the phenomenological analysis.

3. Neutral Current couplings

We can obtain the coupling of the neutral Higgs boson to the SM fermion from Eq. (A20) by doing $f = g$, in this case, it is more convenient to define $Y_{hk}^F \equiv Y_{f^h f^k}^F$ and $X_{hk}^F \equiv X_{f^h f^k}^F$

$$\begin{aligned} Y_{hk}^F &= \left(U_L^F \mathcal{Y}^{1F} U_R^{F\dagger} \right)^{hk} = \left(U_L^F [+ \cos \beta y^{1F} + \sin \beta y^{2F}] U_R^{F\dagger} \right)^{hk} \\ X_{hk}^F &= \left(U_L^F \mathcal{Y}^{2F} U_R^{F\dagger} \right)^{hk} = \left(U_L^F [- \sin \beta y^{1F} + \cos \beta y^{2F}] U_R^{F\dagger} \right)^{hk}. \end{aligned} \quad (\text{A21})$$

For some applications is good to put the Yukawa couplings in terms of the fermion mass. Since Y_{hk}^F is diagonal in the fermion mass eigenstate we can write these Yukawa matrices as follows

$$Y_{hk}^F = \frac{\sqrt{2}}{v} m_k^F \delta_{hk}, \quad (\text{A22})$$

clearing $U_L^F y^{1F} U_R^{F\dagger}$ from the first expression in Eq. (A20) and replacing in the second one, we get

$$X_{hk}^F = -\frac{\sqrt{2}}{v} \tan \beta m_k^F \delta_{hk} + \frac{1}{\cos \beta} \left(U_L^F y^{2F} U_R^{F\dagger} \right)^{hk}, \quad (\text{A23})$$

Contrary case, if we clear $U_L^F y^{2F} U_R^{F\dagger}$ we get

$$X_{hk}^F = \frac{\sqrt{2}}{v} \cot \beta m_k^F \delta_{hk} - \frac{1}{\sin \beta} \left(U_L^F y^{1F} U_R^{F\dagger} \right)^{hk}. \quad (\text{A24})$$

Equations (A23) and (A24) are equivalent, however, their usefulness depends on the model. For $h \neq k$ these identities imply that if y^{2F} is zero (since $\delta_{hk} = 0$), the component $(U_L^F y^{1F} U_R^{F\dagger})_{hk}$ is also zero. From this result, we can conclude that $U_L^F y^{1F} U_R^{F\dagger}$ must be diagonal. This result is also clear from Eq. (A20). These results imply that all the 2HDM types mentioned above avoid flavor changing neutral currents (FCNC).

	X_{cb}^D	$X_{bc}^{U^*}$	$X_{\nu\tau}^{E^*}$	$X_{\tau\nu\tau}^N$
I	$+\cot\beta\frac{\sqrt{2}}{v}V_{CKM}^{cb}m_b$	$+\cot\beta\frac{\sqrt{2}}{v}V_{CKM}^{cb}m_c$	$+\cot\beta\frac{\sqrt{2}}{v}V_{PMNS}^{\tau\nu\tau}m_\tau$	0
II	$-\tan\beta\frac{\sqrt{2}}{v}V_{CKM}^{cb}m_b$	$+\cot\beta\frac{\sqrt{2}}{v}V_{CKM}^{cb}m_c$	$-\tan\beta\frac{\sqrt{2}}{v}V_{PMNS}^{\tau\nu\tau}m_\tau$	0
X	$+\cot\beta\frac{\sqrt{2}}{v}V_{CKM}^{cb}m_b$	$+\cot\beta\frac{\sqrt{2}}{v}V_{CKM}^{cb}m_c$	$-\tan\beta\frac{\sqrt{2}}{v}V_{PMNS}^{\tau\nu\tau}m_\tau$	0
Y	$-\tan\beta\frac{\sqrt{2}}{v}V_{CKM}^{cb}m_b$	$+\cot\beta\frac{\sqrt{2}}{v}V_{CKM}^{cb}m_c$	$+\cot\beta\frac{\sqrt{2}}{v}V_{PMNS}^{\tau\nu\tau}m_\tau$	0

TABLE VII. Yukawa couplings for several 2HDMs in the literature.

4. Charged currents

In order to explain the R_D and R_{D^*} anomalies, flavor violating couplings are needed. We are particularly interested in the effective interaction Lagrangian between a charged Higgs boson and the standard model charged currents. In order to determine the explicit form of the charged current matrices $Y_{g^hfk}^F$ and $X_{g^hfk}^F$, it is convenient to put all in terms of the neutral charged currents

$$Y_{g^hfk}^F = \left(U_L^G \mathcal{Y}^{1F} U_R^{F\dagger} \right)^{hk} = \left(U_L^G U_L^{F\dagger} U_L^F \mathcal{Y}^{1F} U_R^{F\dagger} \right)^{hk} = \left(U_L^G U_L^{F\dagger} Y_{hk}^F \right)^{hk}. \quad (\text{A25})$$

In particular cases this expression means

$$Y_{g^hfk}^F = \left(U_L^G U_L^{F\dagger} \frac{\sqrt{2}}{v} \mathbf{m}^F \right)^{hk} = \begin{cases} \left(V_{CKM} \frac{\sqrt{2}}{v} \mathbf{m}^D \right)^{hk} = \frac{\sqrt{2}}{v} (V_{CKM})^{hk} m_k^D & \text{for } G = U \text{ and } F = D \\ \left(V_{CKM}^\dagger \frac{\sqrt{2}}{v} \mathbf{m}^U \right)^{hk} = \frac{\sqrt{2}}{v} (V_{CKM}^\dagger)^{hk} m_k^U & \text{for } G = D \text{ and } F = U \\ \left(V_{PMNS} \frac{\sqrt{2}}{v} \mathbf{m}^E \right)^{hk} = \frac{\sqrt{2}}{v} (V_{PMNS})^{hk} m_k^E & \text{for } G = N \text{ and } F = E \\ \left(V_{PMNS}^\dagger \frac{\sqrt{2}}{v} \mathbf{m}^N \right)^{hk} = \frac{\sqrt{2}}{v} (V_{PMNS}^\dagger)^{hk} m_k^N & \text{for } G = E \text{ and } F = N \end{cases}.$$

Proceeding in identical way for the couplings to the additional Higgs doublet

$$\begin{aligned} X_{g^hfk}^F &= \left(U_L^G U_L^{F\dagger} X_{hk}^F \right)^{hk} \\ &= -\tan\beta Y_{g^hfk}^F + \frac{1}{\cos\beta} \left(U_L^G y_{2F} U_R^{F\dagger} \right)^{hk} \\ &= +\cot\beta Y_{g^hfk}^F - \frac{1}{\sin\beta} \left(U_L^F y_{1F} U_R^{F\dagger} \right)^{hk}. \end{aligned} \quad (\text{A26})$$

This equation allows determining the couplings for each of the models.

-
- [1] J. P. Lees *et al.* [BaBar Collaboration], Evidence for an excess of $\bar{B} \rightarrow D^{(*)}\tau^-\bar{\nu}_\tau$ decays, Phys. Rev. Lett. **109**, 101802 (2012) [arXiv:1205.5442 [hep-ex]].
- [2] J. P. Lees *et al.* [BaBar Collaboration], Measurement of an Excess of $\bar{B} \rightarrow D^{(*)}\tau^-\bar{\nu}_\tau$ Decays and Implications for Charged Higgs Bosons, Phys. Rev. D **88**, no. 7, 072012 (2013) [arXiv:1303.0571 [hep-ex]].
- [3] M. Huschle *et al.* [Belle Collaboration], Measurement of the branching ratio of $\bar{B} \rightarrow D^{(*)}\tau^-\bar{\nu}_\tau$ relative to $\bar{B} \rightarrow D^{(*)}\ell^-\bar{\nu}_\ell$ decays with hadronic tagging at Belle, Phys. Rev. D **92**, no. 7, 072014 (2015) [arXiv:1507.03233 [hep-ex]].
- [4] Y. Sato *et al.* [Belle Collaboration], Phys. Rev. D **94**, no. 7, 072007 (2016) [arXiv:1607.07923 [hep-ex]].
- [5] S. Hirose [Belle Collaboration], $\bar{B} \rightarrow D^{(*)}\tau^-\bar{\nu}_\tau$ and Related Tauonic Topics at Belle, arXiv:1705.05100 [hep-ex].
- [6] R. Aaij *et al.* [LHCb Collaboration], Measurement of the ratio of branching fractions $\mathcal{B}(\bar{B}^0 \rightarrow D^{*+}\tau^-\bar{\nu}_\tau)/\mathcal{B}(\bar{B}^0 \rightarrow D^{*+}\mu^-\bar{\nu}_\mu)$, Phys. Rev. Lett. **115**, no. 11, 111803 (2015) Erratum: [Phys. Rev. Lett. **115**, no. 15, 159901 (2015)] [arXiv:1506.08614 [hep-ex]].
- [7] R. Aaij *et al.* [LHCb Collaboration], Test of Lepton Flavor Universality by the measurement of the $B^0 \rightarrow D^{*-}\tau^+\nu_\tau$ branching fraction using three-prong τ decays, Phys. Rev. D **97**, no. 7, 072013 (2018) [arXiv:1711.02505 [hep-ex]].

- [8] R. Aaij *et al.* [LHCb Collaboration], Measurement of the ratio of the $B^0 \rightarrow D^{*-}\tau^+\nu_\tau$ and $B^0 \rightarrow D^{*-}\mu^+\nu_\mu$ branching fractions using three-prong τ -lepton decays, Phys. Rev. Lett. **120**, no. 17, 171802 (2018) [arXiv:1708.08856 [hep-ex]].
- [9] G. Caria *et al.* [Belle Collaboration], Measurement of $\mathcal{R}(D)$ and $\mathcal{R}(D^*)$ with a Semileptonic Tagging Method, Phys. Rev. Lett. **124** (2020) no.16, 161803 [arXiv:1910.05864 [hep-ex]].
- [10] S. Hirose *et al.* [Belle Collaboration], Measurement of the τ lepton polarization and $R(D^*)$ in the decay $\bar{B} \rightarrow D^*\tau^-\bar{\nu}_\tau$ with one-prong hadronic τ decays at Belle, Phys. Rev. D **97**, no. 1, 012004 (2018) [arXiv:1709.00129 [hep-ex]].
- [11] S. Hirose *et al.* [Belle Collaboration], Measurement of the τ lepton polarization and $R(D^*)$ in the decay $\bar{B} \rightarrow D^*\tau^-\bar{\nu}_\tau$, Phys. Rev. Lett. **118**, no. 21, 211801 (2017) [arXiv:1612.00529 [hep-ex]].
- [12] Y. S. Amhis *et al.* [HFLAV Collaboration], Averages of b -hadron, c -hadron, and τ -lepton properties as of 2018, arXiv:1909.12524 [hep-ex].
- [13] For updated results see HFLAV average of $R(D^{(*)})$ for Spring 2019 in <https://hflav-eos.web.cern.ch/hflav-eos/semi/spring19/html/RDsDsstar/RDRDs.html>.
- [14] R. Aaij *et al.* [LHCb Collaboration], Measurement of the ratio of branching fractions $\mathcal{B}(B_c^+ \rightarrow J/\psi\tau^+\nu_\tau)/\mathcal{B}(B_c^+ \rightarrow J/\psi\mu^+\nu_\mu)$, Phys. Rev. Lett. **120**, no. 12, 121801 (2018) [arXiv:1711.05623 [hep-ex]].
- [15] A. Abdesselam *et al.* [Belle Collaboration], Measurement of the D^{*-} polarization in the decay $B^0 \rightarrow D^{*-}\tau^+\nu_\tau$, arXiv:1903.03102 [hep-ex].
- [16] R. Watanabe, New Physics effect on $B_c \rightarrow J/\psi\tau\bar{\nu}$ in relation to the $R_{D^{(*)}}$ anomaly, Phys. Lett. B **776**, 5 (2018) [arXiv:1709.08644 [hep-ph]].
- [17] M. Tanaka and R. Watanabe, New physics in the weak interaction of $\bar{B} \rightarrow D^{(*)}\tau\bar{\nu}$, Phys. Rev. D **87**, no. 3, 034028 (2013) [arXiv:1212.1878 [hep-ph]].
- [18] A. K. Alok, D. Kumar, S. Kumbhakar and S. U. Sankar, D^* polarization as a probe to discriminate new physics in $\bar{B} \rightarrow D^*\tau\bar{\nu}$, Phys. Rev. D **95**, no. 11, 115038 (2017) [arXiv:1606.03164 [hep-ph]].
- [19] D. Bigi and P. Gambino, Revisiting $B \rightarrow D\ell\nu$, Phys. Rev. D **94**, 094008 (2016). [arXiv:1606.08030 [hep-ph]]
- [20] F. U. Bernlochner, Z. Ligeti, M. Papucci, and D. J. Robinson, Combined analysis of semileptonic B decays to D and D^* : $R(D^{(*)})$, $|V_{cb}|$, and new physics, Phys. Rev. D **95**, 115008 (2017). arXiv:1703.05330 [hep-ph]
- [21] S. Jaiswal, S. Nandi, and S. K. Patra, Extraction of $|V_{cb}|$ from $B \rightarrow D^{(*)}\ell\nu_\ell$ and the Standard Model predictions of $R(D^{(*)})$, JHEP **1712**, 060 (2017) [arXiv:1707.09977 [hep-ph]].
- [22] D. Bigi, P. Gambino, and S. Schacht, $R(D^*)$, $|V_{cb}|$, and the Heavy Quark Symmetry relations between form factors, JHEP **11**, 061 (2017). [arXiv:1707.09509 [hep-ph]]
- [23] P. Gambino, M. Jung and S. Schacht, The V_{cb} puzzle: An update, Phys. Lett. B **795**, 386-390 (2019) [arXiv:1905.08209 [hep-ph]].
- [24] S. Jaiswal, S. Nandi and S. K. Patra, [arXiv:2002.05726 [hep-ph]].
- [25] S. Kamali, New physics in inclusive semileptonic B decays including nonperturbative corrections, Int. J. Mod. Phys. A **34**, no. 06n07, 1950036 (2019) [arXiv:1811.07393 [hep-ph]].
- [26] E. Kou *et al.* [Belle-II Collaboration], The Belle II Physics Book, PTEP **2019**, no. 12, 123C01 (2019) Erratum: [PTEP **2020**, no. 2, 029201 (2020)] [arXiv:1808.10567 [hep-ex]].
- [27] P. Asadi and D. Shih, Maximizing the Impact of New Physics in $b \rightarrow c\tau\nu$ Anomalies, Phys. Rev. D **100**, no. 11, 115013 (2019) [arXiv:1905.03311 [hep-ph]].
- [28] C. Murgui, A. Peñuelas, M. Jung and A. Pich, Global fit to $b \rightarrow c\tau\nu$ transitions, JHEP **1909**, 103 (2019) [arXiv:1904.09311 [hep-ph]].
- [29] R. Mandal, C. Murgui, A. Peñuelas and A. Pich, The role of right-handed neutrinos in $b \rightarrow c\tau\bar{\nu}$ anomalies, arXiv:2004.06726 [hep-ph].
- [30] K. Cheung, Z. R. Huang, H. D. Li, C. D. Lü, Y. N. Mao and R. Y. Tang, Revisit to the $b \rightarrow c\tau\nu$ transition: in and beyond the SM, arXiv:2002.07272 [hep-ph].
- [31] S. Sahoo and R. Mohanta, Investigating the role of new physics in $b \rightarrow c\tau\bar{\nu}$ transitions, arXiv:1910.09269 [hep-ph].
- [32] R. X. Shi, L. S. Geng, B. Grinstein, S. Jäger and J. Martin Camalich, Revisiting the new-physics interpretation of the $b \rightarrow c\tau\nu$ data, JHEP **1912**, 065 (2019) [arXiv:1905.08498 [hep-ph]].
- [33] D. Bardhan and D. Ghosh, B -meson charged current anomalies: The post-Moriond 2019 status, Phys. Rev. D **100** (2019) no.1, 011701 [arXiv:1904.10432 [hep-ph]].
- [34] M. Blanke, A. Crivellin, S. de Boer, T. Kitahara, M. Moscati, U. Nierste and I. Nisandzic, Impact of polarization observables and $B_c \rightarrow \tau\nu$ on new physics explanations of the $b \rightarrow c\tau\nu$ anomaly, Phys. Rev. D **99**, no.7, 075006 (2019) [arXiv:1811.09603 [hep-ph]].
- [35] M. Blanke, A. Crivellin, T. Kitahara, M. Moscati, U. Nierste and I. Nisandzic, Addendum to “Impact of polarization observables and $B_c \rightarrow \tau\nu$ on new physics explanations of the $b \rightarrow c\tau\nu$ anomaly”, Phys. Rev. D **100**, 035035 (2019) [arXiv:1905.08253 [hep-ph]].
- [36] A. K. Alok, D. Kumar, S. Kumbhakar and S. Uma Sankar, Solutions to $R_D-R_{D^*}$ in light of Belle 2019 data, Nucl. Phys. B **953**, 114957 (2020) [arXiv:1903.10486 [hep-ph]].
- [37] Z. R. Huang, Y. Li, C. D. Lu, M. A. Paracha and C. Wang, Footprints of New Physics in $b \rightarrow c\tau\nu$ Transitions, Phys. Rev. D **98**, no.9, 095018 (2018) [arXiv:1808.03565 [hep-ph]].
- [38] A. Crivellin, C. Greub and A. Kokulu, Explaining $B \rightarrow D\tau\nu$, $B \rightarrow D^*\tau\nu$ and $B \rightarrow \tau\nu$ in a 2HDM of type III, Phys. Rev. D **86**, 054014 (2012) [arXiv:1206.2634 [hep-ph]].
- [39] A. Crivellin, A. Kokulu and C. Greub, Flavor-phenomenology of two-Higgs-doublet models with generic Yukawa structure, Phys. Rev. D **87**, no. 9, 094031 (2013) [arXiv:1303.5877 [hep-ph]].

- [40] A. Celis, M. Jung, X. Q. Li and A. Pich, Sensitivity to charged scalars in $B \rightarrow D^{(*)}\tau\nu_\tau$ and $B \rightarrow \tau\nu_\tau$ decays, JHEP **1301**, 054 (2013) [arXiv:1210.8443 [hep-ph]].
- [41] A. Celis, M. Jung, X. Q. Li and A. Pich, Scalar contributions to $b \rightarrow c(u)\tau\nu$ transitions, Phys. Lett. B **771**, 168 (2017) [arXiv:1612.07757 [hep-ph]].
- [42] P. Ko, Y. Omura and C. Yu, $B \rightarrow D^*\tau\nu$ and $B \rightarrow \tau\nu$ in chiral U(1)' models with flavored multi Higgs doublets, JHEP **1303**, 151 (2013) [arXiv:1212.4607 [hep-ph]].
- [43] J. Hernandez-Sanchez, S. Moretti, R. Noriega-Papaqui and A. Rosado, Off-diagonal terms in Yukawa textures of the Type-III 2-Higgs doublet model and light charged Higgs boson phenomenology, JHEP **1307**, 044 (2013) [arXiv:1212.6818 [hep-ph]].
- [44] A. Crivellin, J. Heeck and P. Stoffer, A perturbed lepton-specific two-Higgs-doublet model facing experimental hints for physics beyond the Standard Model, Phys. Rev. Lett. **116**, no. 8, 081801 (2016) [arXiv:1507.07567 [hep-ph]].
- [45] J. M. Cline, Scalar doublet models confront τ and b anomalies, Phys. Rev. D **93**, no. 7, 075017 (2016) [arXiv:1512.02210 [hep-ph]].
- [46] T. Enomoto and R. Watanabe, Flavor constraints on the Two Higgs Doublet Models of Z_2 symmetric and aligned types, JHEP **1605**, 002 (2016) [arXiv:1511.05066 [hep-ph]].
- [47] L. Dhargyal, $R(D^{(*)})$ and $\mathcal{B}r(B \rightarrow \tau\nu_\tau)$ in a Flipped/Lepton-Specific 2HDM with anomalously enhanced charged Higgs coupling to τ/b , Phys. Rev. D **93**, no. 11, 115009 (2016) [arXiv:1605.02794 [hep-ph]].
- [48] R. Martinez, C. F. Sierra and G. Valencia, Beyond $\mathcal{R}(D^{(*)})$ with the general type-III 2HDM for $b \rightarrow c\tau\nu$, Phys. Rev. D **98**, no. 11, 115012 (2018) [arXiv:1805.04098 [hep-ph]].
- [49] L. Wang, J. M. Yang and Y. Zhang, Probing a pseudoscalar at the LHC in light of $R(D^{(*)})$ and muon g-2 excesses, Nucl. Phys. B **924**, 47 (2017) [arXiv:1610.05681 [hep-ph]].
- [50] C. H. Chen and T. Nomura, Charged-Higgs on $R_{D^{(*)}}$, τ polarization, and FBA, Eur. Phys. J. C **77**, no. 9, 631 (2017) [arXiv:1703.03646 [hep-ph]].
- [51] S. Iguro, Y. Omura and M. Takeuchi, Test of the $R(D^{(*)})$ anomaly at the LHC, Phys. Rev. D **99**, no. 7, 075013 (2019) [arXiv:1810.05843 [hep-ph]].
- [52] S. Iguro and K. Tobe, $R(D^{(*)})$ in a general two Higgs doublet model, Nucl. Phys. B **925**, 560 (2017) [arXiv:1708.06176 [hep-ph]].
- [53] A. Arbey, F. Mahmoudi, O. Stal and T. Stefaniak, Status of the Charged Higgs Boson in Two Higgs Doublet Models, Eur. Phys. J. C **78**, no. 3, 182 (2018) [arXiv:1706.07414 [hep-ph]].
- [54] C. H. Chen and T. Nomura, Charged Higgs boson contribution to $B_q^- \rightarrow \ell\bar{\nu}$ and $\bar{B} \rightarrow (P, V)\ell\bar{\nu}$ in a generic two-Higgs doublet model, Phys. Rev. D **98**, no. 9, 095007 (2018) [arXiv:1803.00171 [hep-ph]].
- [55] K. Hagiwara, M. M. Nojiri and Y. Sakaki, CP violation in $B \rightarrow D\tau\nu_\tau$ using multipion tau decays, Phys. Rev. D **89**, no. 9, 094009 (2014) [arXiv:1403.5892 [hep-ph]].
- [56] J. P. Lee, $B \rightarrow D^{(*)}\tau\nu_\tau$ in the 2HDM with an anomalous τ coupling, Phys. Rev. D **96**, no.5, 055005 (2017) [arXiv:1705.02465 [hep-ph]].
- [57] S. Iguro and Y. Omura, Status of the semileptonic B decays and muon g-2 in general 2HDMs with right-handed neutrinos, JHEP **1805**, 173 (2018) [arXiv:1802.01732 [hep-ph]].
- [58] S. P. Li, X. Q. Li, Y. D. Yang and X. Zhang, $R_{D^{(*)}}$, $R_{K^{(*)}}$ and neutrino mass in the 2HDM-III with right-handed neutrinos, JHEP **1809**, 149 (2018) [arXiv:1807.08530 [hep-ph]].
- [59] R. Alonso, B. Grinstein and J. Martin Camalich, Lifetime of B_c^- Constrains Explanations for Anomalies in $B \rightarrow D^{(*)}\tau\nu$, Phys. Rev. Lett. **118**, no. 8, 081802 (2017) [arXiv:1611.06676 [hep-ph]].
- [60] A. G. Akeroyd and C. H. Chen, Constraint on the branching ratio of $B_c \rightarrow \tau\bar{\nu}$ from LEP1 and consequences for $R(D^{(*)})$ anomaly, Phys. Rev. D **96**, no. 7, 075011 (2017) [arXiv:1708.04072 [hep-ph]].
- [61] S. Iguro, T. Kitahara, Y. Omura, R. Watanabe and K. Yamamoto, D^* polarization vs. $R_{D^{(*)}}$ anomalies in the leptoquark models, JHEP **1902**, 194 (2019) [arXiv:1811.08899 [hep-ph]].
- [62] P. Asadi, M. R. Buckley and D. Shih, It's all right(-handed neutrinos): a new W' model for the $R_{D^{(*)}}$ anomaly, JHEP **1809**, 010 (2018) [arXiv:1804.04135 [hep-ph]].
- [63] P. Asadi, M. R. Buckley and D. Shih, Asymmetry Observables and the Origin of $R_{D^{(*)}}$ Anomalies, Phys. Rev. D **99**, no. 3, 035015 (2019) [arXiv:1810.06597 [hep-ph]].
- [64] Z. Ligeti, M. Papucci and D. J. Robinson, New Physics in the Visible Final States of $B \rightarrow D^{(*)}\tau\nu$, JHEP **1701** (2017) 083 [arXiv:1610.02045 [hep-ph]].
- [65] D. J. Robinson, B. Shakya and J. Zupan, Right-handed neutrinos and $R(D^{(*)})$, JHEP **1902** (2019) 119 [arXiv:1807.04753 [hep-ph]].
- [66] A. Greljo, D. J. Robinson, B. Shakya and J. Zupan, $R(D^{(*)})$ from W' and right-handed neutrinos, JHEP **1809** (2018) 169 [arXiv:1804.04642 [hep-ph]].
- [67] A. Azatov, D. Barducci, D. Ghosh, D. Marzocca and L. Ubaldi, Combined explanations of B-physics anomalies: the sterile neutrino solution, JHEP **1810** (2018) 092 [arXiv:1807.10745 [hep-ph]].
- [68] J. Heeck and D. Teresi, Pati-Salam explanations of the B-meson anomalies, JHEP **1812** (2018) 103 [arXiv:1808.07492 [hep-ph]].
- [69] K. S. Babu, B. Dutta and R. N. Mohapatra, A theory of $R(D^*, D)$ anomaly with right-handed currents, JHEP **1901** (2019) 168 [arXiv:1811.04496 [hep-ph]].

- [70] X. G. He and G. Valencia, Lepton universality violation and right-handed currents in $b \rightarrow c\tau\nu$, Phys. Lett. B **779** (2018) 52 [arXiv:1711.09525 [hep-ph]].
- [71] J. D. Gómez, N. Quintero and E. Rojas, Charged current $b \rightarrow c\tau\bar{\nu}_\tau$ anomalies in a general W' boson scenario, Phys. Rev. D **100** (2019) no.9, 093003 [arXiv:1907.08357 [hep-ph]].
- [72] M. Algueró, S. Descotes-Genon, J. Matias and M. Novoa Brunet, Symmetries in $B \rightarrow D^*\ell\nu$ angular observables, arXiv:2003.02533 [hep-ph].
- [73] R. Dutta, A. Bhol and A. K. Giri, Effective theory approach to new physics in $b \rightarrow u$ and $b \rightarrow c$ leptonic and semileptonic decays, Phys. Rev. D **88**, no.11, 114023 (2013) [arXiv:1307.6653 [hep-ph]].
- [74] R. Dutta and A. Bhol, $B_c \rightarrow (J/\psi, \eta_c)\tau\nu$ semileptonic decays within the standard model and beyond,” Phys. Rev. D **96**, no.7, 076001 (2017) [arXiv:1701.08598 [hep-ph]].
- [75] R. Dutta, Exploring R_D , R_{D^*} and $R_{J/\psi}$ anomalies, [arXiv:1710.00351 [hep-ph]].
- [76] R. Dutta and N. Rajeev, Signature of lepton flavor universality violation in $B_s \rightarrow D_s\tau\nu$ semileptonic decays, Phys. Rev. D **97**, no.9, 095045 (2018) [arXiv:1803.03038 [hep-ph]].
- [77] P. A. Zyla *et al.* [Particle Data Group], Review of Particle Physics, to be published in Prog. Theor. Exp. Phys. 2020, 083C01 (2020).
- [78] M. Tanaka, Charged Higgs effects on exclusive semitauonic B decays, Z. Phys. C **67**, 321 (1995) [hep-ph/9411405].
- [79] M. Tanaka and R. Watanabe, Tau longitudinal polarization in $B \rightarrow D\tau\nu$ and its role in the search for charged Higgs boson, Phys. Rev. D **82**, 034027 (2010) [arXiv:1005.4306 [hep-ph]].
- [80] W. S. Hou, Enhanced charged Higgs boson effects in $B^- \rightarrow \tau\bar{\nu}, \mu\bar{\nu}$ and $b \rightarrow \tau\bar{\nu} + X$, Phys. Rev. D **48**, 2342 (1993).
- [81] J. F. Kamenik and F. Mescia, $B \rightarrow D\tau\nu$ Branching Ratios: Opportunity for Lattice QCD and Hadron Colliders, Phys. Rev. D **78**, 014003 (2008) [arXiv:0802.3790 [hep-ph]].
- [82] U. Nierste, S. Trine and S. Westhoff, Charged-Higgs effects in a new $B \rightarrow D\tau\nu$ differential decay distribution, Phys. Rev. D **78**, 015006 (2008) [arXiv:0801.4938 [hep-ph]].
- [83] S. Fajfer, J. F. Kamenik and I. Nisandzic, On the $B \rightarrow D^*\tau\bar{\nu}_\tau$ Sensitivity to New Physics, Phys. Rev. D **85**, 094025 (2012) [arXiv:1203.2654 [hep-ph]].
- [84] M. Misiak and M. Steinhauser, Weak radiative decays of the B meson and bounds on M_{H^\pm} in the Two-Higgs-Doublet Model, Eur. Phys. J. C **77**, no. 3, 201 (2017) [arXiv:1702.04571 [hep-ph]].